leukonychia, or porcelain nails, resulting from mutations in PLCD1. Am J Hum Genet 2011;88:839–44.

Kouzarides T, Ziff E. The role of the leucine zipper in the fos–jun interaction. Nature 1988;336:646–51.

Leppard BJ, Sanderson KV, Wells RS. Hereditary trichilemmal cysts. Hereditary pilar cysts. Clin Exp Dermatol 1977;2:23–32.

Loh PR, Danecek P, Palamara PF, Fuchsberger C, Reshef Y A, K Finucane H, et al. Reference-based phasing using the Haplotype Reference Consortium panel. Nat Genet 2016;48:1443–8.

MacArthur DG, Balasubramanian S, Frankish A, Huang N, Morris J, Walter K, et al. A systematic survey of loss-of-function variants in human protein-coding genes [published correction appears in Science 2012;336:6079]. Science 2012;335:823–8.

Nakamura M, Schneider MR, Schmidt-Ullrich R, Paus R. Mutant laboratory mice with abnormalities in hair follicle morphogenesis, cycling, and/or structure: an update. J Dermatol Sci 2013;69:6–29.

Nguyen TA, Debnath J. Unconventional secretion: cargo channeling by TMED10. Cell Res 2020;30:713–4.

Rafnar T, Sulem P, Stacey SN, Geller F, Gudmundsson J, Sigurdsson A, et al. Sequence variants at the tert-CLPTM1L locus associate with many cancer types. Nat Genet 2009;41:221–7.

Seidenari S, Pellacani G, Nasti S, Tomasi A, Pastorino L, Ghiorzo P, et al. Hereditary trichilemmal cysts: a proposal for the assessment of diagnostic clinical criteria. Clin Genet 2013;84:65–9.

Yousaf A, Tallman R, Katzman S, Brady C, Fang W, Kolodney MS. Genotype-phenotype correlation in trichilemmal cysts. J Invest Dermatol 2021;141:2983–5.

Zheng X, Davis JW. SAIGEgds-an efficient statistical tool for large-scale PheWAS with mixed models. Bioinformatics 2021;37:728–30.

A Genome-Wide Scan on Individual Typology Angle Found Variants at *SLC24A2* Associated with Skin Color Variation in Chinese Populations

JID Open

Journal of Investigative Dermatology (2022) **142,** 1217–1223; doi:10.1016/j.jid.2021.07.186

TO THE EDITOR

Skin pigmentation functions as a shield to prevent UV damage to the DNA of epidermal cells. A good number of GWASs on skin color variation or skin photosensitivity have been conducted that discovered a large number of associated loci (Ganguly et al., 2019). Polymorphisms/mutations at these loci have been used to study the molecular type of skin color for individuals from different continental groups (Chen et al., 2021) and have been associated with various forms of albinism (Marçon and Maia, 2019), loss of photoprotection, and increased rates of photoaging (Liu et al., 2016). However, there have been surprisingly few GWASs conducted in East Asian populations, likely owing to the presumption of a low skin color variation in East Asians (Rawofi et al., 2017). The question regarding the presence of East Asian–specific skin color alleles remains to be answered. Individual typology angle (ITA°) is a quantitative skin color measurement based on the colorimetric parameters of the L*a*b* system (Chardon et al., 1991). The validity of ITA° in serving as an objective skin color measurement has been extensively evaluated with regard to its correlations with constitutive pigmentation, the geographical distribution of skin pigmentation, and biological markers of UV-induced erythema (Del Bino and Bernerd, 2013). Despite the wide use of ITA° in clinical dermatology, few genetic studies had adopted it as the measurement of skin color.

In this study, we report a GWAS of ITA° in Chinese, followed by replications in Chinese and Latin Americans. The discovery sample included a total of 6,964 individuals of Chinese origin from two cohorts: the Jidong cohort (n = 5,034) and the National Survey of Physical Traits cohort (n = 1,930). Studies in these cohorts were approved by the Ethics Committee of Kailuan General Hospital of Tangshan City and the Medical Ethics Committee, Staff Hospital, Jidong Oilfield Branch, China National Petroleum Corporation in July 2013 (approval number 2013 YILUNZI1) as well as the Ethics Committees of Fudan University (14117) and the Shanghai Institutes for Biological Sciences (ER-SIBS-261410). The replication sample included a total of 2,053 individuals from two cohorts: the Taizhou longitudinal cohort of Chinese origin (n = 1,787) and the Colombian cohort of Latin American origin (n = 266). The Taizhou longitudinal cohort study was conducted with the approval of the Ethics Committee of Fudan University (Ethics Research Approval 85), Shanghai, China, and the Colombian cohort study was conducted with the approval of the bioethics committee of the Odontology Faculty at the University of Antioquia (CONCEPTO 01-2013). All participants provided written informed consent. For the discovery cohorts, sample characteristics and phenotyping details are provided in Supplementary Materials and Methods (Supplementary Table S1 and Figure 1a and b). In brief, we derived ITA° from high-resolution portrait photos, which were processed using an in-house pipeline, involving a face detector, automated facial landmarking, cheek segmentation, and color analysis. In a subgroup of 50 randomly selected samples, the ITA° derived from the portrait photos was highly correlated with the ITA° measured by a spectrophotometer ($r = 0.94$, $P = 4.42 \times 10^{-24}$, Supplementary Figure S1). The Chardon skin color type (Chardon et al., 1991), as defined by ITA° cutoffs, was fairly concordant with human perception (Kappa = 0.47). Although dark skins were not

Abbreviation: ITA°, individual typology angle

Accepted manuscript published online 25 September 2021; corrected proof published online 9 November 2021

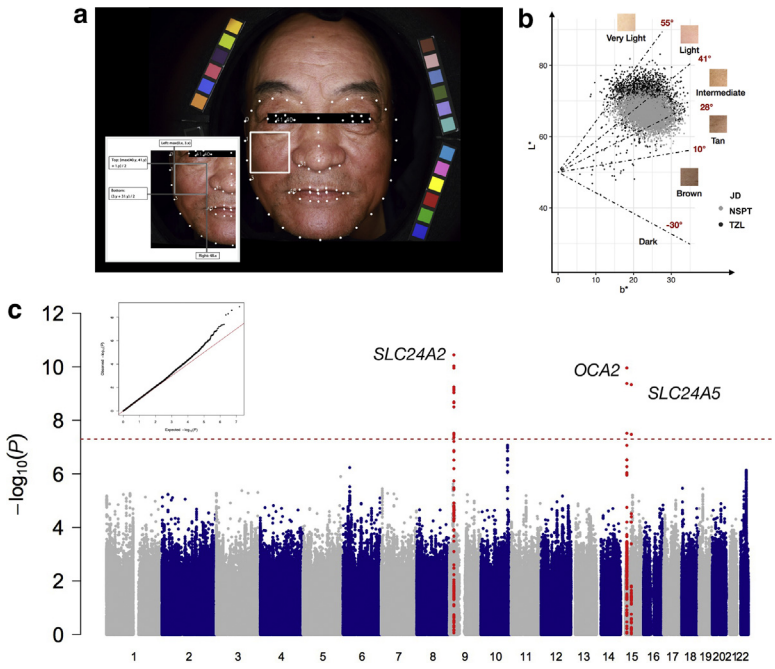

Figure 1. GWASs for skin color in Chinese populations. (**a**) The face detection module returned the locations of 68 facial landmarks (white points), and a fixed area on the cheek (white rectangle) was detected on the basis of seven facial landmarks. The participant has consented to the publication of his image. (**b**) ITA° was derived from the fixed area. Samples were classified into five skin color types on the basis of ITA° according to Chardon's definition. **(c)** Manhattan plot of the meta-analysis results for facial skin color from the GWASs (JD and NSPT, total N = 6,964). The $-\log_{10}$ *P*-values for association were plotted for all SNPs according to their physical positions (genome-build GRCh38.p13). The red line was corresponding to the threshold for genome-wide significance ($P = 5 \times 10^{-8}$). Genome-wide significant and nominal significant ($P = 1 \times 10^{-6}$) SNPs were shown in Supplementary Tables S2 and S3, respectively. ITA°, individual typology angle; JD, Jidong cohort; NSPT, National Survey of Physical Traits cohort.

seen and very light (1.51%) and brown (0.27%) skins were rarely seen in our Chinese samples, ITA° did show a substantial variance (Var = 8.03, mean = 35.95, minimum = −26.36, maximum = 68.42) across light (23.41%), intermediate (59.69%), and tan (15.12%) categories. Females had significant lighter skin than males ($\beta = 6.18$, $P = 9.22 \times 10^{-270}$) and aging increased coloration ($\beta = -0.22$, $P = 8.08 \times 10^{-244}$), which were consistent with previous observations (Tan et al., 2020). Z-transformed ITA° was used in the subsequent genetic association analysis (Supplementary Figure S2).

In the discovery stage of the study, we conducted a genome-wide inverse variance, a fixed-effect meta-analysis of two GWASs, which were independently conducted in the Jidong cohort and the National Survey of Physical Traits cohort, totaling 6,964 Chinese individuals. No evidence of population substratification or genome inflation was detected ($\lambda = 0.99$, Figure 1c). The meta-analysis identified a total of 19 SNPs at three genomic loci showing genome-wide significant association with z-transformed ITA° (Supplementary Table S2), including one previously unreported locus on 9p21.3 (*SLC24A2*) and two previously known loci on 15q12.6 (*OCA2*) and 15p21.1 (*SLC24A5*).

The locus at 9p21.3, as the most significant signal over the genome, contained a total of 14 significant SNPs, where the lead SNP (rs10122939) was an intron variant of *SLC24A2* (Figure 2a). The derived G allele showed a skin darkening effect reaching genome-wide significance in the Jidong cohort ($\beta = -0.10$, $P = 1.29 \times 10^{-9}$), nominal significance in the National Survey of Physical Traits cohort ($\beta = -0.07$, $P = 4.71 \times 10^{-3}$), and further enhanced significance in the meta-analysis ($\beta = -0.09$, $P = 3.61 \times 10^{-11}$). This association was also genome-wide significant for the original ITA° without z-transformation ($\beta = -1.89$, $P = 7.28 \times 10^{-10}$). No genome-wide significant association signal was observed at 9p21.3 after conditioning on the genotype of the lead SNP rs10122939 (Supplementary Figure S3). The G allele of rs10122939 was highly prevalent in East Asians (our sample: f = 0.34; in CHB of the 1000 Genomes Project: f = 0.29) but was rare in Europeans (in EUR of 1000 Genomes Project, f = 0.004, Figure 2b), which may explain the failure of previous European GWASs in detecting its effect (other SNPs in linkage disequilibrium showed the same pattern, Supplementary Table S2). A series of population genetic analyses did not reveal significant evidence for positive selection surrounding rs10122939 at 9p21.3 (Supplementary Figure S4).

The other two loci have been previously associated with skin color. On chromosome 15q12.6, two well-known East Asian–specific missense variants rs1800414 (His615Arg) and rs74653330 (Ala481Thr) of *OCA2* (Edwards et al., 2010; Yang et al., 2016) showed genome-wide significant association with ITA°, where the derived C allele of rs1800414 and T allele of rs74653330 had a skin-lightening effect ($P = 1.11 \times 10^{-10}$ and $P = 3.05 \times 10^{-8}$, respectively; Supplementary Table S2 and Supplementary Figure S5a and b). Both alleles were nearly absent outside of East Asia (Supplementary Figure S5c and d). On chromosome 15p21.1, we confirmed the well-known effect of a missense variant rs1426654 of *SLC24A5*, of which the derived A allele had low frequency but a large skin-lightening effect

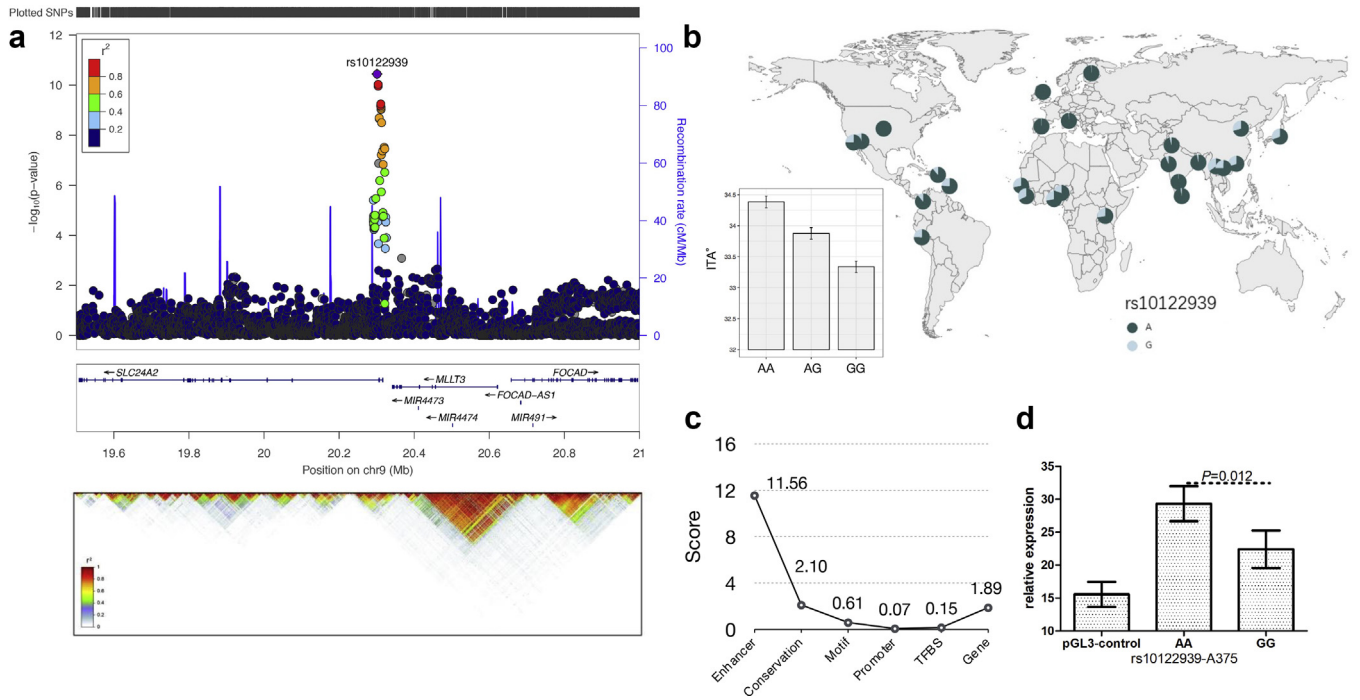

Figure 2. A locus at 9p21.3 was associated with skin color in Chinese populations. (**a**) Regional association plot for the significantly associated region on chromosome 9p21.3 consisting of *SLC24A2*. Increasing color intensities represented higher levels of linkage disequilibrium (r^2) with rs10122939. (**b**) Geographical distribution of the minor allele frequencies for rs10122939 in 2,504 multiethnic individuals from the 1000 Genome Project. The effect allele (G) showed a skin-darkening effect. (**c**) The top SNP rs10122939 was annotated as an enhancer using 3DSNP. (**d**) Luciferase reporter assays confirmed that the transcriptional activity of the enhancer containing the rs10122939 ancestral A allele was significantly higher than that of the corresponding-derived G allele in the A375 cell line. A similar trend was observed but did not reach the significant level in HEK293 (Supplementary Figure S7). chr, chromosome; HEK293, human embryonic kidney 293; ITA°, individual typology angle; TFBS, transcription factor binding sites.

($P = 4.64 \times 10^{-10}$, Supplementary Table S2 and Supplementary Figure S6).

We then looked up a total of 9,183 SNPs from four recently published large GWASs of skin/hair/eye pigmentation traits (Adhikari et al., 2019; Hysi et al., 2018; Simcoe et al., 2021; Visconti et al., 2018). A total of 151 SNPs at 13 loci showed nominally significant ($P < 0.01$) association, but except those in or close to *OCA2* and *SLC24A5* genes, none survived strict Bonferroni correction of multiple testing ($P < 0.05/9{,}183$; Supplementary Table S4).

To replicate the finding at 9p21.3, we tested the association between rs10122939 and ITA° in an additional Chinese cohort from Taizhou (Taizhou longitudinal cohort, n = 1,787) and in a Latin American cohort from Colombia (n = 266). The effect of rs10122939 was successfully replicated at nominal significance, and the G allele also showed a skin-darkening effect in both replication cohorts (Taizhou longitudinal cohort: $\beta = -0.09$, $P = 5.96 \times 10^{-3}$, Colombian: $\beta = -0.26$, $P = 3.89 \times 10^{-2}$). A meta-analysis of all samples further enhanced the significance level of this association ($P = 2.13 \times 10^{-13}$).

To further investigate the potential functions of rs10122939, we conducted a function annotation analysis using the quantitative scoring system embedding the 3DSNP database (Lu et al., 2017), which revealed significant evidence for rs10122939 serving as an enhancer of *SLC24A2* (Figure 2c). We further performed the luciferase report assays to experimentally validate this finding. The transcriptional activity of the enhancer containing the rs10122939 ancestral A allele was significantly higher than that of the corresponding derived G allele in the A375 cell line (*t*-test $P = 0.012$, Figure 2d). This pattern would predict less *SLC24A2* production for the derived G allele carriers. Future studies may consider in vivo gene editing experiments to further investigate the pigmentation effect of *SLC24A2*. Unlike the well-known skin color genes *SLC24A5* and *SLC45A2*, this SLC family gene *SLC24A2* is not expressed in the skin but rather in the brain and adrenal, mainly involved in neuronal activity (Haque and Moon, 2018; Zhou et al., 2020). It has been recently reported that neuronal activity induced by acute stress can drive a rapid and permanent loss of melanocyte stem cells, which leads up to stress-induced hair greying (Zhang et al., 2020). A possible hypothesis could be that *SLC24A2* moderates neuronal activity that influences melanocyte stem cells, eventually causing changes in skin color. Alternatively, *SLC24A2* may change the innervation of the skin and affect ITA° through altered skin thickness or other relevant characteristics. This hypothesis is particularly attractive because we did observe a positive correlation between ITA° and transepidermal water loss ($P = 4.12 \times 10^{-9}$), a phenotype thought to be strongly associated with skin thickness (Bargo et al., 2013). The rs10122939 SNP is also associated with transepidermal water loss ($P = 0.01$) (Supplementary Figure S8 and Supplementary Materials and Methods).

In conclusion, this is a meaningful skin color GWAS in well-sized Chinese populations. We identified an intron variant of *SLC24A2* (rs10122939) as a

previously unreported East Asian–European differentiating polymorphism involved in skin color variation. The underlying cellular mechanism is to be explored.

Data availability statement

Summary statistics for all analyzed variants for the Jidong Study and the National Survey of Physical Traits can be viewed at NODE under accession number OEP001341 or directly at http://www.biosino.org/node/project/detail/OEP001341 and accessed by submitting a request for data access. Data usage shall be in full compliance with the Regulations on Management of Human Genetic Resources in China. Individual genotype and phenotype data cannot be shared owing to Institutional Review Board restrictions on privacy concerns. All other relevant data supporting the key findings of this study are available within the letter and Supplementary Materials or from the corresponding author on reasonable request.

ORCIDs

Fudi Wang: http://orcid.org/0000-0002-0208-3343
Qi Luo: http://orcid.org/0000-0002-6988-2051
Yan Chen: http://orcid.org/0000-0002-6873-8648
Yu Liu: http://orcid.org/0000-0001-7110-127X
Ke Xu: http://orcid.org/0000-0002-0408-1659
Kaustubh Adhikari: http://orcid.org/0000-0001-5825-4191
Xiyang Cai: http://orcid.org/0000-0002-3868-5426
Jialin Liu: http://orcid.org/0000-0003-4065-5397
Yi Li: http://orcid.org/0000-0002-2448-9176
Xuyang Liu: http://orcid.org/0000-0002-0871-8979
Luis-Miguel Ramirez-Aristeguieta: http://orcid.org/0000-0002-0961-5824
Ziyu Yuan: http://orcid.org/0000-0003-1434-0383
Yong Zhou: http://orcid.org/0000-0001-5221-8026
Fu-feng Li: http://orcid.org/0000-0002-0566-3589
Binghua Jiang: http://orcid.org/0000-0003-4526-2031
Li Jin: http://orcid.org/0000-0001-9201-2321
Andrés Ruiz-Linares: http://orcid.org/0000-0001-8372-1011
Zhaohui Yang: http://orcid.org/0000-0003-0958-4439
Fan Liu: http://orcid.org/0000-0001-9241-8161
Sijia Wang: http://orcid.org/0000-0001-6961-7867

CONFLICT OF INTEREST

The authors state no conflict of interest.

ACKNOWLEDGMENTS

This work has received funding from the Strategic Priority Research Program of the Chinese Academy of Sciences (XDB38020400 and XDB38010400), the National Key Research and Development Project (2018YFC0910403), Shanghai Municipal Science and Technology Major Project (2017SHZDZX01), the National Basic Research Program (2015FY111700), the CAS Interdisciplinary Innovation Team project, Beijing Advanced Discipline Fund, the National Natural Science Foundation of China (81930056, 91651507, 32070579, 31771393, and 31601016), the Open Project of Key Laboratory of Genomic and Precision Medicine of the CAS, State Key Laboratory of Genetic Resources and Evolution grant (GREKF20-13), the Leverhulme Trust (F/07 134/DF), BBSRC (BB/I021213/1), the Excellence Initiative of Aix-Marseille University - A*MIDEX (a French Investissements d'Avenir programme, 2RUIZLRE/RHRE/ID18HRU201 and 20-07874), the Scientific and Technology Committee of Shanghai Municipality (18490750300), Ministry of Science and Technology of China (2020YFE0201600), and the 111 Project (B13016), Santander Research and Scholarship Award, and Bogue Fellowship from University College London. Correspondences regarding the luciferase assays and population comparative analyses should be addressed to ZY (yangzhaohui415@163.com) and FL (liufan@big.ac.cn), respectively.

AUTHOR CONTRIBUTIONS

Conceptualization: FW, SW; Data Curation: FW; Formal Analysis: FW, QL, YC, YLiu, XC, JL, YLi, ZY; Funding Acquisition: ZY, FL, SW; Investigation: FW, QL, KX, XL, ZY; Methodology: FW, QL; Project Administration: FW, FL, SW; Resources: LMRA, ZY, FFL, YZ, BJ, LJ, ARL, SW; Software: FW, QL; Supervision: FL, SW; Validation: YC, KA; Visualization: FW, FL, SW; Writing - Original Draft Preparation: FW, FL; Writing - Review and Editing: QL, YC, YLiu, KA, XC, JL, YLi, ZY, SW

Fudi Wang[1,2,3,19], Qi Luo[2,19], Yan Chen[4,5,6], Yu Liu[2], Ke Xu[7], Kaustubh Adhikari[8,9], Xiyang Cai[2], Jialin Liu[4,5,6], Yi Li[4,5,6], Xuyang Liu[10], Luis-Miguel Ramirez-Aristeguieta[11], Ziyu Yuan[12,13], Yong Zhou[14], Fu-Feng Li[15], Binghua Jiang[7], Li Jin[2,12,13], Andres Ruiz-Linares[16,17,9], Zhaohui Yang[7,20], Fan Liu[4,5,6,20] and Sijia Wang[2,18,*,20]

[1]Department of Skin & Cosmetic Research, Shanghai Skin Disease Hospital, Shanghai, China; [2]CAS Key Laboratory of Computational Biology, CAS-MPG Partner Institute for Computational Biology, Shanghai Institute of Nutrition and Health, University of Chinese Academy of Sciences, Chinese Academy of Sciences, Shanghai, China; [3]Department of Science, Inertia Shanghai Biotechnology Co., Ltd, Shanghai, China; [4]Key Laboratory of Genomic and Precision Medicine, Beijing Institute of Genomics, Chinese Academy of Sciences, Beijing, China; [5]School of Future Technology, University of Chinese Academy of Sciences, Beijing, China; [6]China National Center for Bioinformation, Beijing, China; [7]Academy of Medicine Science, Zhengzhou University, Zhengzhou, China; [8]School of Mathematics and Statistics, Faculty of Science, Technology, Engineering and Mathematics, The Open University, Milton Keynes, United Kingdom; [9]UCL Genetics Institute, Department of Genetics, Evolution and Environment, University College London, London, United Kingdom; [10]Yunnan Key Laboratory of Primate Biomedical Research, Institute of Primate Translational Medicine, Kunming University of Science and Technology, Kunming, China; [11]QST Lab, Faculty of Odontology, University of Antioquia, Medellin, Colombia; [12]Fudan University Taizhou Institute of Health Sciences, Taizhou, China; [13]State Key Laboratory of Genetic Engineering, Human Phenome Institute, and School of Life Sciences, Fudan University, Shanghai, China; [14]Clinical Research Institute, Shanghai General Hospital, School of Medicine, Shanghai Jiao Tong University, Shanghai, China; [15]Basic Medical Department, Shanghai University of Traditional Chinese Medicine, Shanghai, China; [16]Ministry of Education Key Laboratory of Contemporary Anthropology and Collaborative Innovation Center of Genetics and Development, School of Life Sciences and Human Phenome Institute, Fudan University, Shanghai, China; [17]UMR 7268 ADES, Centre national de la recherche scientifique (CNRS), EFS, Faculté de Médecine Timone, Aix-Marseille Université, Marseille, France; and [18]Center for Excellence in Animal Evolution and Genetics, Chinese Academy of Sciences, Kunming, China

[19]These authors contributed equally to this work.

[20]These authors contributed equally to this work.

[*]Corresponding author e-mail: wangsijia@picb.ac.cn

SUPPLEMENTARY MATERIAL

Supplementary material is linked to the online version of the paper at www.jidonline.org, and at https://doi.org/10.1016/j.jid.2021.07.186.

REFERENCES

Bargo PR, Walston ST, Chu M, Seo I, Kollias N. Non-invasive assessment of tryptophan fluorescence and confocal microscopy provide information on skin barrier repair dynamics beyond TEWL. Exp Dermatol 2013;22:18–23.

Chardon A, Cretois I, Hourseau C. Skin colour typology and suntanning pathways. Int J Cosmet Sci 1991;13:191–208.

Chen Y, Branicki W, Walsh S, Nothnagel M, Kayser M, Liu F, et al. The impact of correlations between pigmentation phenotypes and underlying genotypes on genetic prediction of pigmentation traits. Forensic Sci Int Genet 2021;50:102395.

Del Bino S, Bernerd F. Variations in skin colour and the biological consequences of ultraviolet radiation exposure. Br J Dermatol 2013;169(Suppl. 3):33–40.

Edwards M, Bigham A, Tan J, Li S, Gozdzik A, Ross K, et al. Association of the OCA2 polymorphism His615Arg with melanin content in east Asian populations: further evidence of convergent evolution of skin pigmentation. PLoS Genet 2010;6:e1000867.

Ganguly K, Saha T, Saha A, Dutta T, Banerjee S, Sengupta D, et al. Meta-analysis and prioritization of human skin pigmentation-associated GWAS-SNPs using ENCODE data-based web-tools. Arch Dermatol Res 2019;311:163–71.

Haque MN, Moon IS. Stigmasterol upregulates immediate early genes and promotes neuronal cytoarchitecture in primary hippocampal neurons as revealed by transcriptome analysis. Phytomedicine 2018;46:164–75.

Hysi PG, Valdes AM, Liu F, Furlotte NA, Evans DM, Bataille V, et al. Genome-wide association meta-analysis of individuals of European ancestry

identifies new loci explaining a substantial fraction of hair color variation and heritability [published correction appears in Nat Genet 2019;51:1190]. Nat Genet 2018;50:652–6.

Liu F, Hamer MA, Deelen J, Lall JS, Jacobs L, van Heemst D, et al. The MC1R gene and youthful looks. Curr Biol 2016;26:1213–20.

Lu Y, Quan C, Chen H, Bo X, Zhang C. 3DSNP: a database for linking human noncoding SNPs to their three-dimensional interacting genes. Nucleic Acids Res 2017;45:D643–9.

Marçon CR, Maia M. Albinism: epidemiology, genetics, cutaneous characterization, psychosocial factors. An Bras Dermatol 2019;94:503–20.

Rawofi L, Edwards M, Krithika S, Le P, Cha D, Yang Z, et al. Genome-wide association study of pigmentary traits (skin and iris color) in individuals of East Asian ancestry. PeerJ 2017;5:e3951.

Simcoe M, Valdes A, Liu F, Furlotte NA, Evans DM, Hemani G, et al. Genome-wide association study in almost 195,000 individuals identifies 50 previously unidentified genetic loci for eye color. Sci Adv 2021;7:eabd1239.

Tan Y, Wang F, Fan G, Zheng Y, Li B, Li N, et al. Identification of factors associated with minimal erythema dose variations in a large-scale population study of 22 146 subjects. J Eur Acad Dermatol Venereol 2020;34:1595–600.

Visconti A, Duffy DL, Liu F, Zhu G, Wu W, Chen Y, et al. Genome-wide association study in 176,678 Europeans reveals genetic loci for tanning response to sun exposure. Nat Commun 2018;9:1684.

Yang Z, Zhong H, Chen J, Zhang X, Zhang H, Luo X, et al. A genetic mechanism for convergent skin lightening during recent human evolution. Mol Biol Evol 2016;33:1177–87.

Zhang B, Ma S, Rachmin I, He M, Baral P, Choi S, et al. Hyperactivation of sympathetic nerves drives depletion of melanocyte stem cells. Nature 2020;577:676–81.

Zhou XG, He H, Wang PJ. A critical role for miR-135-a5p-mediated regulation of SLC24A2 in neuropathic pain. Mol Med Rep 2020;22:2115–22.

Read-Through for Nonsense Mutations in Type XVII Collagen–Deficient Junctional Epidermolysis Bullosa

Journal of Investigative Dermatology (2022) **142,** 1217–1227; doi:10.1016/j.jid.2021.09.018

TO THE EDITOR

Junctional epidermolysis bullosa (JEB) is caused by mutations in genes encoding adhesion proteins, such as laminin 332, type XVII collagen (COL17), integrin α6β4, or integrin α3. The absence of COL17 leads to intermediate JEB that manifests with generalized skin blisters, chronic wounds, hair loss, nail loss or dystrophy, and enamel hypoplasia (Has et al., 2020). There is no cure, and no experimental therapy has been developed for JEB with COL17 deficiency (Prodinger et al., 2020). About 20% of the *COL17A1* pathogenic variants are nonsense mutations leading to the absence of COL17. Studies of genotype–phenotype correlations showed that small amounts of partially functional COL17 have biological relevance and translate into mild phenotypes (Condrat et al., 2018; Kroeger et al., 2019, 2017; Ruzzi et al., 2001). In this study, we address the question of whether translational read-through–inducing drugs (TRIDs) have an effect on *COL17A1* nonsense mutations and represent a therapeutic option to alleviate disease severity.

After written informed consent, keratinocytes (KCs) from seven patients with JEB with *COL17A1* nonsense pathogenic variant were studied (Supplementary Materials and Methods). *COL17A1* mRNA was expressed in all cells with various degrees of decay in cases 3, 5, 6, and 7. Four cell lines were completely devoid of COL17 (cases 1, 2, 4, and 7), whereas three of them (cases 3, 5, and 6) expressed low levels of COL17 compared with normal KCs (Figure 1a). This was due either to a second heterozygous splicing mutation (cases 3 and 6) or to natural alternative splicing of exon 33 containing the pathogenic variant p.R795* (case 5) (Ruzzi et al., 2001). We focused on the COL17-negative KCs carrying the homozygous mutations p.W464*, p.R688*, p.R1226*, and p.S140* and treated them with the TRIDs gentamicin, paromomycin, G418, amlexanox, or PTC124. Whereas amlexanox and PTC124 had no effect on any of the mutant KCs, differential response to aminoglycosides was observed (Figure 1b). The p.W464* mutant KCs showed a robust and dose-dependent response to gentamicin (125–1,000 μg/ml), paromomycin (500–2,000 μg/ml), and G418 (1–10 μg/ml) (Figure 1c). The amount of COL17 expressed after treatment with 500 μg/ml gentamicin was much smaller than that of normal cells (Figure 2a). The effect of gentamicin, paromomycin, and G418 on the p.R688* mutant KCs was subtle, and COL17 was clearly detectable when the highest TRIDs concentrations were used (Figure 1c). The other two mutations, p.R1226* and p.S140*, did not respond to any TRIDs (Figure 1b and data not shown).

Next, we asked how long COL17 was able to persist in JEB KCs after a single treatment with gentamicin. Mutant p.W464* KCs showed the highest COL17 level 2 days after the addition of 500 μg/ml gentamicin. The COL17 amount decreased progressively and was barely detectable 6 days after treatment (Figure 2b).

To investigate whether COL17 expressed after read-through in JEB KCs was functional and able to be deposited at the dermal–epidermal junction, we analyzed its presence in cell culture media and in epidermal equivalents. The 120 kDa COL17 shed ectodomain was found in conditioned media of p.W464* mutant KCs after G418 treatment, suggesting that insertion of a cognate amino acid did not alter

Abbreviations: COL17, type XVII collagen; JEB, junctional epidermolysis bullosa; KC, keratinocyte; TRID, translational read-through–inducing drug

Accepted manuscript published online 18 October 2021; corrected proof published online 5 November 2021

SUPPLEMENTARY MATERIALS AND METHODS

Study populations

The Jidong cohort. The Jidong cohort is a community-based, long-term observational cohort study to evaluate health-related risk factors. The baseline data were collected from 2013 to 2014 in the Staff Hospital, Jidong Oilfield Branch, China. Approval was obtained from the Ethics Committee of Kailuan General Hospital of Tangshan City and the Medical Ethics Committee, Staff Hospital, Jidong Oilfield Branch, China National Petroleum Corporation in July 2013 (approval number 2013 YILUNZI1). The approval had been renewed in 2018. To date, 9,078 individuals aged >18 years have been enrolled after excluding individuals who were unable or unwilling to participate. Written informed consent was obtained from all participants. This study included a total of 5,601 individuals (2,512 men and 3,089 women, aged 31–87 years) who paid the return visit in 2018. The facial photograph and blood samples were collected in the Staff Hospital at the same time.

The National Survey of Physical Traits cohort. The National Survey of Physical Traits cohort (NSPT) is a population-based prospective cohort study to explore the environmental and genetic factors associated with physical traits and diseases. The NSPT cohort study was conducted with the official approval of the Ethics Committees of Fudan University (14117) and the Shanghai Institutes for Biological Sciences (ER-SIBS-261410). The NSPT totally collected samples of 3,565 Han Chinese individuals (1,320 men and 2,245 women, aged 17–83 years) in 2015–2018 from three sites (i.e., Taizhou, Nanning, and Zhengzhou). All individuals provided written informed consent. Portrait photos of 1,930 individuals (705 men and 1,225 women, aged 18–79 years) were collected in accordance with phenotyping standard operating procedure. Therefore, only 1,930 individuals were included in this study.

The Taizhou longitudinal cohort. The Taizhou longitudinal cohort study is a long-term observational cohort study to explore the environmental and genetic risk factors for common and noncommunicable diseases. This research program was conducted with the approval of the Ethics Committee of Fudan University (Ethics Research Approval 85), Shanghai, China. The detailed characteristics have been described before (Wang et al., 2009). Our replication set included 1,787 healthy Han Chinese with portrait photos, aged 31–85 years.

Colombian cohort. The Colombian cohort collected data from participants of several Latin American countries to study the genetics of normal variation in physical appearance. For the genetic analysis of individual typology angle (ITA°), 266 participants were recruited in the city of Medellin, Colombia. Ethical approval was obtained from the bioethics committee of the Odontology Faculty at the University of Antioquia (Medellin, Colombia) (CONCEPTO 01-2013). The age of the participants was between 18–50 years, with an average of 27 years.

Phenotyping

All participants were asked not to take part in vigorous exercise an hour before their study visit, not to wear make-up, and to refrain from alcohol and tobacco use 24 hours before the visit. All photographs were taken in a confined space with stabilized light-emitting diode light source. Besides, all participants wore a shawl to help give consistent light illumination. A Canon 70D digital camera (lens: Canon EF 40 mm f/2.8; Canon, Tokyo, Japan) was used for all subjects without the flash. The facial photograph for each participant consisted of a frontal facial shot with the eyes closed and no facial expression. The resolution of the photographs was 300 dpi.

This study adopted ITA° as a quantitative measurement of skin color, which was derived from high-resolution portrait photos. ITA° is a quantitative variable designed for measuring skin pigmentation on the basis of colorimetric parameters. ITA° could be used to classify skin types, that is, very light (ITA° > 55), light (41 ~ 55), intermediate (28 ~ 41), tan (10 ~ 28), brown (−30 ~ 10), and dark (<−30) (Chardon et al., 1991). It has been shown that the ITA°-based skin color classification is physiologically relevant (Del Bino and Bernerd, 2013).

Portrait photos were processed using an in-house developed facial skin color quantification pipeline, which involves a face detector, automated facial landmarking, cheek segmentation, and color analysis.

The face detection was achieved by the get_frontal_face_detector function from the C++ library Dlib (King, 2009). This function returns an object detector that is configured to find human faces that are looking more or less toward the camera, and the detector is composed of a linear classifier combined with classic Histogram of Oriented Gradients features (Dalal and Triggs, 2005), an image pyramid, and the sliding window detection scheme (Sullivan and Su, 2014). The face landmarking was achieved by the shape_predictor function from the C++ library Dlib on the basis of the face region detected by the get_frontal_face_detector. This predictor was created by training an ensemble of regression trees for face alignment on the iBUG 300-W face landmark dataset (Sagonas et al., 2016; Sagonas et al., 2013a, 2013b). It takes an image of a human face as input and identifies the locations of 68 facial landmarks including, the corners of the mouth and eyes, the tip of the nose, and edges of cheeks (Figure 1a).

For each side of the face, the pipeline automatically outlines a rectangle to segment the cheek part according to preselected anatomical landmarks in such a way that the rectangle contains the cheek-surrounding landmarks with the minimal horizontal and vertical distances between the landmarks (Figure 1a). After the segmentation, we manually examined the scope of the rectangles to exclude the confounding margins that incorporate photographing background and human hair. For the right cheek, the CIELAB (ISO, 2007) L, a and b values of all segmented pixels were obtained and converted to ITA° as $\mathrm{ITA}^{\circ} = \arctan\frac{L-50}{b} \times \frac{180}{\pi}$, and the mean ITA° was calculated to represent the facial skin color of a portrait. Because ITA° values were not subject to the normal distribution both in the Jidong cohort and the NSPT cohort (Supplementary Figure S2a and b), we applied Z-transformed ITA° in further analysis.

For quality control purposes, additional measures were obtained in a subgroup of 50 randomly selected photographs. These included accessing skin colorimetric parameters on the right cheek using a spectrophotometer

(Skin Colorimeter CL 400, Courage+Khazaka Electronics GmbH, Cologne, Germany) and four skin color types (very light, light, intermediate, and tan) perceived by an investigator according to the Chardon skin color type (Chardon et al., 1991). Note that dark skin color types were absent in our Chinese sample. Intermethod reliability was evaluated with the Kappa statistic. No significant difference in ITA^{o} was detected between the left and right cheeks (*t*-test $P = 0.13$). Chardon's skin color type showed a high degree of concordance with the perceived skin color type as well as with the spectrophotometer values (Supplementary Figure S1b–d).

For phenotyping in the Taizhou longitudinal cohort, the photos were taken with a Canon 70D digital camera (lens: Canon EF 40 mm f/2.8). The rest of the procedures (i.e., automated facial landmarking, cheek segmentation, and color analysis) were the same as those used in the discovery cohorts.

For the Colombian cohort, ITA^{o} was measured on the forehead. Owing to the smaller sample size, outlier values on either tail of the ITA^{o} were excluded (values ≤ -3 or ≥ 54). Z-transformed ITA^{o} was used for the analysis.

Among 1,887 subjects in the NSPT cohort, we also collected the transepidermal water loss measurement. Transepidermal water loss was measured on the cheek using Tewameter TM 300 of Courage+Khazaka Electronics GmbH (median [interquartile range], g/h/m^2 = 10.60 [8.20–13.90]).

Genotyping

For both the Jidong and NSPT cohorts, genomic DNA was extracted from blood samples using the MagPure Blood DNA KF Kit. All samples were genotyped using the Illumina Infinium Global Screening Array (Illumina, San Diego, CA) consisting of about 710,000 SNPs. We implemented exclusion criteria for quality control using PLINK, version 1.9 (Chang et al., 2015). In detail, we excluded subjects with >5% missing data, the duplicated subjects, and subjects that failed the X-chromosome sex concordance check or had ethnic information incompatible with their genetic information. We excluded SNPs that had >2% missing data, SNPs with a minor allele frequency <1%, and the ones that failed the Hardy–Weinberg deviation test ($P < 1 \times 10^{-5}$). Imputation was performed using the 1000 Genomes Project phase 3 as the reference panel. The chip genotype data were firstly phased using SHAPEIT3 (O'Connell et al., 2016), and IMPUTE2 was then used to impute genotypes (Howie et al., 2009). SNPs with an imputation quality score (INFO) <0.6, minor allele frequency <0.01, or a missing rate >0.01 were eliminated from further analyses. Finally, 8,039,700 SNPs passed quality control and were used for further analyses.

For Taizhou longitudinal cohort, blood samples were collected, and DNA was extracted. All samples were genotyped using the Illumina HumanOmniZhongHua-8 chip (Illumina), which interrogates 894,517 SNPs. After quality control with PLINK, version 1.9, the genotype data were phased using SHAPEIT and were imputed using IMPUTE2 with the 1000 Genomes Project phase 3.

Blood samples were collected from the participants in the Colombian cohort. DNA was extracted and genotyped on the Illumina Infinium Global Screening Array. After quality control using PLINK, version 1.9, 511,848 SNPs were retained. The genotype data were then phased using SHAPEIT2 and imputed using IMPUTE2, with the 1000 Genomes Project phase 3 as the reference panel. Genotype data for SNP rs10122939 were obtained from the imputed dataset.

Statistical analysis

GWASs and meta-analysis. GWASs were separately conducted in the Jidong and NSPT cohorts on Z-transformed ITA^{o} values using software package PLINK (Chang et al., 2015) where additive allele effects were tested in linear models adjusted for covariates (age, sex, sampling locations, and the top four genomic principal components). GWAS outputs were combined using inverse variance fixed-effect meta-analysis as implemented in METAL (Willer et al., 2010). *P*-values $\leq 5 \times 10^{-8}$ from the meta-analysis were considered genome-wide significant. The inflation factor was estimated close to 1.0 ($\lambda = 0.995$) and not further considered. GWAS results were visualized using Manhattan plots, Q–Q plots. Regional linkage disequilibrium plots and association plots were generated using Haploview and LocusZoom (Barrett et al., 2005; Pruim et al., 2010). For the association analysis in the replication cohorts, additive models were used, with age, sex, and five principal components of genotypes as covariates.

In the Taizhou longitudinal cohort and the Colombian cohort, genetic principal components were calculated from the chip genotype data. After quality control, an association test between SNP rs10122939 and Z-transformed ITA^{o} values was conducted using PLINK, including age, sex, and five genetic principal components as covariates.

Candidate gene analysis. To compare our GWAS results with previous GWAS findings related to skin color, we conducted an examination for a list of 11,384 SNPs identified by recently large sample GWAS for tanning response to sun exposure (Visconti et al., 2018), skin pigmentation (Adhikari et al., 2019), hair color (Hysi et al., 2018), and eye color (Simcoe et al., 2021). Of 11,384 SNPs, 9,183 were available in our GWAS results. SNPs with *P*-values smaller than the Bonferroni-corrected threshold of 0.05/9,183 (1.09×10^{-6}) in our GWAS results were considered significant.

Genetic diversity and signatures of positive selection

To detect the signatures of positive selection, we used two statistics commonly adopted in population genetics, including the fixed index (F_{ST}) and integrated haplotype score (iHS). F_{ST} measures the proportion of genetic diversity caused by differences in allele frequencies between populations that is potentially resulted from divergent natural selection (Holsinger and Weir, 2009). We used genome-wide complex trait analysis (Yang et al., 2011) to derive genome-wide F_{ST} analysis for 10 pairs of groups—pairwise among African, East Asian, European, American, and South Asian—on the basis of the genotype data of samples from the 1000 Genome Project. The empirical significance cutoff was set to the values of the top 1% and top 5% of F_{ST} in the corresponding pairs of the population in the whole genome. iHS is an integration of extended haplotype homozygosity statistics to highlight the recent positive selection mutations that have not yet reached a fixed level. Larger values indicated adaptation to selection

pressure in the most recent stage of evolution (Sabeti et al., 2002; Voight et al., 2006). First, We used the selscan software (Szpiech and Hernandez, 2014) to calculate the iHS scores of SNPs on the basis of genotype data from the five populations, including African, East Asian, European, American, and South Asian of the 1000 Genome Project. The absolute iHS scores of the top 1% and 5% of all SNPs in these 22 randomly selected regions for each population were used as the empirical significance cutoff of the corresponding population. Then, we calculated the iHS scores of SNPs within 200 kb upstream and downstream of the lead SNP we identified, and the iHS absolute score represents the selection intensity.

Functional test using a dual-luciferase reporter assay

We amplified a 115 bp fragment (GRCh38.p13) of *SLC24A2* by PCR from genomic DNA of two homozygous individuals with respect to the corresponding genotypes rs10122939 (AA and GG) using primers tailed with *Kpn* I and *Xho* I restriction sites for rs10122939 and directionally subcloned them into the pGL3-promoter expression vector (Promega, Madison, WI). We verified all recombinant clones by sequencing. A375 melanoma cells lines and human embryonic kidney 293 cell lines were routinely cultured, transfected, and incubated overnight at 37 °C in 5% carbon dioxide. A375 and human embryonic kidney 293 cells were cultured in high-glucose DMEM (Corning, Corning, NY) with 10% fetal bovine serum (Gibco, Waltham, MA). Transient transfection assays were conducted in these cells using the Lipofectamine 2000 transfection reagent (Invitrogen, Waltham, MA). All assays were performed with a minimum of four replicates. After 48 hours of incubation, we collected the cells and measured luciferase activity using the Dual-Luciferase Reporter Assay System (Beyotime, Shanghai, China).

SUPPLEMENTARY REFERENCES

Adhikari K, Mendoza-Revilla J, Sohail A, Fuentes-Guajardo M, Lampert J, Chacón-Duque JC, et al. A GWAS in Latin Americans highlights the convergent evolution of lighter skin pigmentation in Eurasia. Nat Commun 2019;10:358.

Barrett JC, Fry B, Maller J, Daly MJ. Haploview: analysis and visualization of LD and haplotype maps. Bioinformatics 2005;21:263–5.

Chang CC, Chow CC, Tellier LC, Vattikuti S, Purcell SM, Lee JJ. Second-generation PLINK: rising to the challenge of larger and richer datasets. GigaScience 2015;4:7.

Chardon A, Cretois I, Hourseau C. Skin colour typology and suntanning pathways. Int J Cosmet Sci 1991;13:191–208.

Dalal N, Triggs B. Histograms of oriented gradients for human detection. Paper presented at: 2005 IEEE Computer Society Conference on Computer Vision and Pattern Recognition 20–25 June 2005;—San Diego, CA.

Del Bino S, Bernerd F. Variations in skin colour and the biological consequences of ultraviolet radiation exposure. Br J Dermatol 2013;169(Suppl. 3):33–40.

Holsinger KE, Weir BS. Genetics in geographically structured populations: defining, estimating and interpreting F(ST). Nat Rev Genet 2009;10:639–50.

Howie BN, Donnelly P, Marchini J. A flexible and accurate genotype imputation method for the next generation of genome-wide association studies. PLoS Genet 2009;5:e1000529.

Hysi PG, Valdes AM, Liu F, Furlotte NA, Evans DM, Bataille V, et al. Genome-wide association meta-analysis of individuals of European ancestry identifies new loci explaining a substantial fraction of hair color variation and heritability [published correction appears in Nat Genet 2019;51:1190]. Nat Genet 2018;50:652–6.

ISO. CIE standard colorimetric observers international organization for standardization. ISO 11664–1:2007 colorimetry – Part 1; 2007.

King DE. Dlib-ml: A machine learning toolkit. J Mach Learn Res 2009;10:1755–8.

O'Connell J, Sharp K, Shrine N, Wain L, Hall I, Tobin M, et al. Haplotype estimation for biobank-scale data sets. Nat Genet 2016;48:817–20.

Pruim RJ, Welch RP, Sanna S, Teslovich TM, Chines PS, Gliedt TP, et al. LocusZoom: regional visualization of genome-wide association scan results. Bioinformatics 2010;26:2336–7.

Sabeti PC, Reich DE, Higgins JM, Levine HZ, Richter DJ, Schaffner SF, et al. Detecting recent positive selection in the human genome from haplotype structure. Nature 2002;419:832–7.

Sagonas C. Tzimiropoulos G, Zafeiriou S, Pantic M. 300 faces in-the-wild challenge: The first facial landmark localization challenge. In: Proceedings of the 2013 IEEE International Conference on Computer Vision Workshops (ICCV-W); 2013a.

Sagonas C. Tzimiropoulos G, Zafeiriou S, Pantic M. A semi-automatic methodology for facial landmark annotation. Proceedings of the 2013 IEEE International Conference Computer Vision and Pattern Recognition Workshops (CVPR-W), 5th Workshop on Analysis and Modeling of Faces and Gestures (AMFG 2013); 2013b.

Sagonas C, Antonakos E, Tzimiropoulos G, Zafeiriou S, Pantic M. 300 faces in-the-wild challenge: database and results. Image Vis Comput 2016;47:3–18.

Simcoe M, Valdes A, Liu F, Furlotte NA, Evans DM, Hemani G, et al. Genome-wide association study in almost 195,000 individuals identifies 50 previously unidentified genetic loci for eye color. Sci Adv 2021;7:eabd1239.

Sullivan V, Su J. One millisecond face alignment with an ensemble of regression trees. In: IEEE Conference on Computer Vision and Pattern Recognition; 2014. p. 1867–74.

Szpiech ZA, Hernandez RD. selscan: an efficient multithreaded program to perform EHH-based scans for positive selection. Mol Biol Evol 2014;31:2824–7.

Visconti A, Duffy DL, Liu F, Zhu G, Wu W, Chen Y, et al. Genome-wide association study in 176,678 Europeans reveals genetic loci for tanning response to sun exposure. Nat Commun 2018;9:1684.

Voight BF, Kudaravalli S, Wen X, Pritchard JK. A map of recent positive selection in the human genome [published correction appears in PLoS Biol 2006;4:e154] [published correction appears in PLoS Biol 2007;5:e147]. PLoS Biol 2006;4:e72.

Wang X, Lu M, Qian J, Yang Y, Li S, Lu D, et al. Rationales, design and recruitment of the Taizhou Longitudinal Study. BMC Public Health 2009;9:223.

Willer CJ, Li Y, Abecasis GR. METAL: fast and efficient meta-analysis of genomewide association scans. Bioinformatics 2010;26:2190–1.

Yang J, Lee SH, Goddard ME, Visscher PM. GCTA: a tool for genome-wide complex trait analysis. Am J Hum Genet 2011;88:76–82.

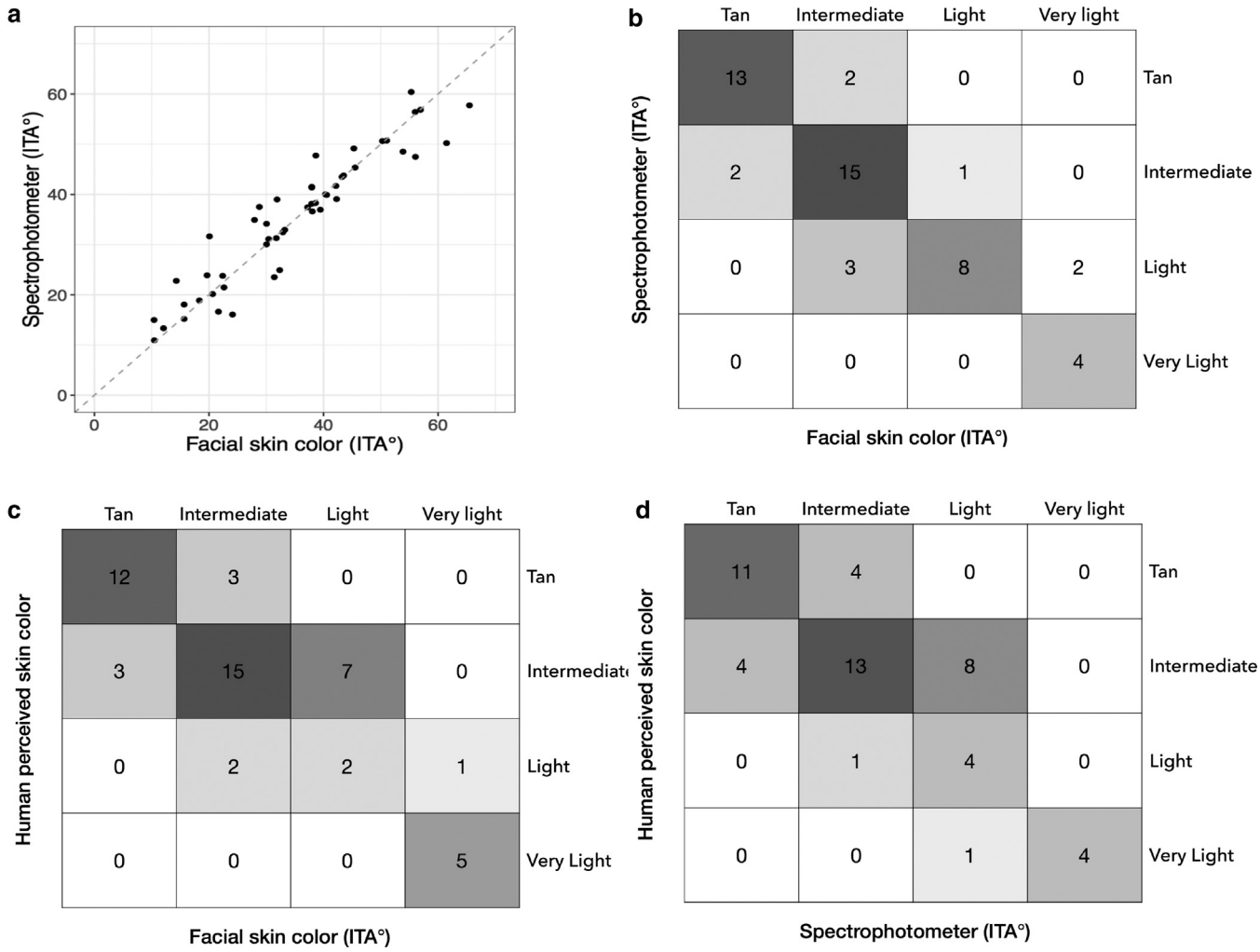

Supplementary Figure S1. Scatter plot and confusion matrices of skin color measurements. (**a**) Scatter plot of portrait-based ITA° and spectrophotometer ITA°. (**b**) Confusion matrices of Chardon skin color types derived from portrait-based ITA° versus those derived from spectrophotometer ITA°. (**c**) Chardon skin color types derived from portrait-based ITA° versus human perceived skin color and (**d**) human perceived skin color versus Chardon skin color types derived from spectrophotometer ITA°. ITA°, individual typology angle.

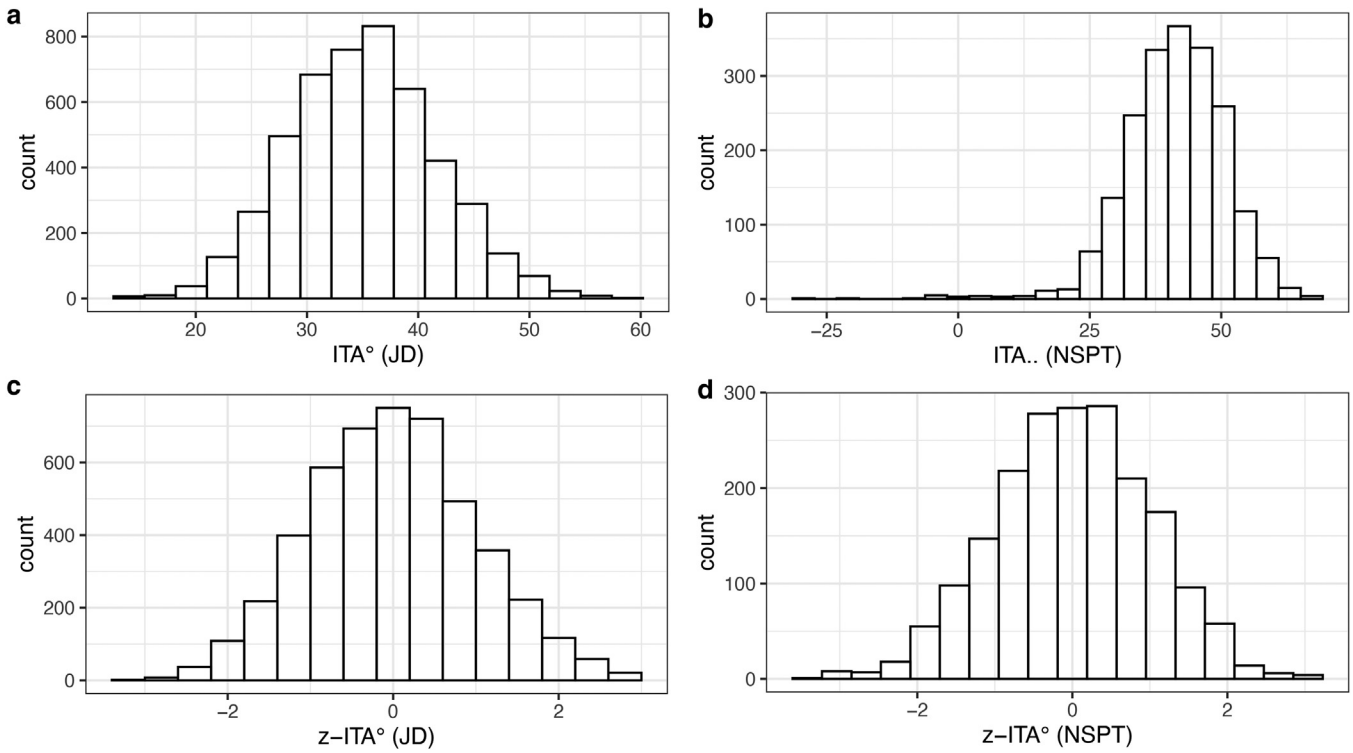

Supplementary Figure S2. Histogram of ITA° in JD and NSPT. (**a, b**) ITA° values were not subject to the normal distribution both in JD and NSPT. (**c, d**) Histogram of z-ITA° in JD and NSPT, respectively. ITA°, individual typology angle; JD, Jidong cohort; NSPT, National Survey of Physical Traits cohort.

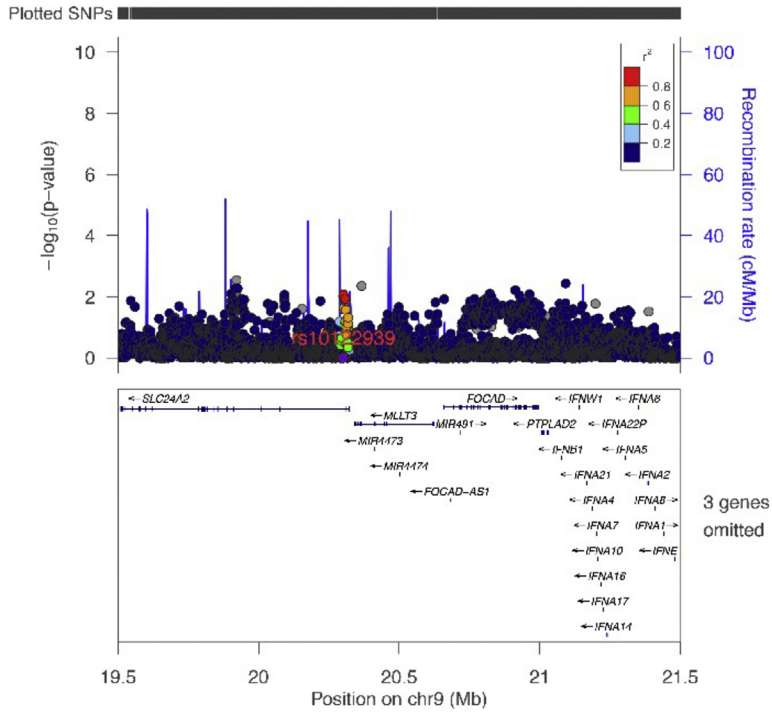

Supplementary Figure S3. Regional association for the significantly associated region on *SLC24A2* after conditioning the leading SNP.

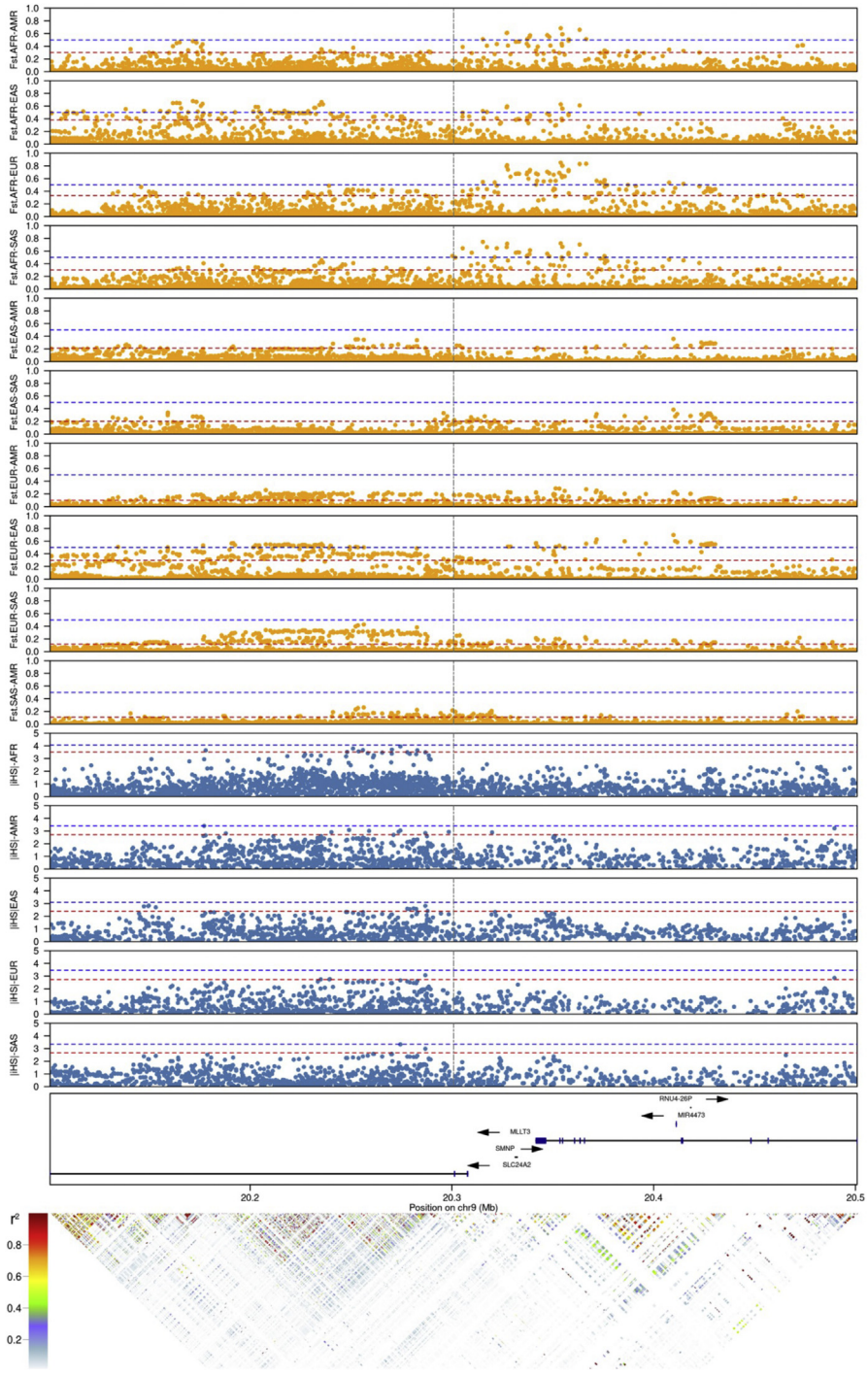

Supplementary Figure S4. Lack of signals of local positive selection for the genome region within 200 kb upstream and downstream of the lead SNP rs10122939. We used F_{ST} and |iHS| statistics between and within EUR. AFR, AMR, SAS, and EAS population samples from the 1000 Genomes Project. Top 1% and 5% statistics cutoff were displayed using dotted lines with corresponding blue and red colors. The location of lead SNP rs10122939 was shown with vertical dotted lines. The gene annotations were based on the latest annotation for hg38 version of the genomic data from the NCBI database. The genomic region of LD plot was consistent with the upside plots. LD ($r^2 > 0.05$) was calculated using the genodata of Europeans obtained from the 1000 Genome Project. AFR, African; AMR, American; EAS, East Asian; EUR, European; F_{ST}, fixed index; iHS, integrated haplotype score; LD, linkage disequilibrium; NCBI, National Center for Biotechnology Information; SAS, South Asian.

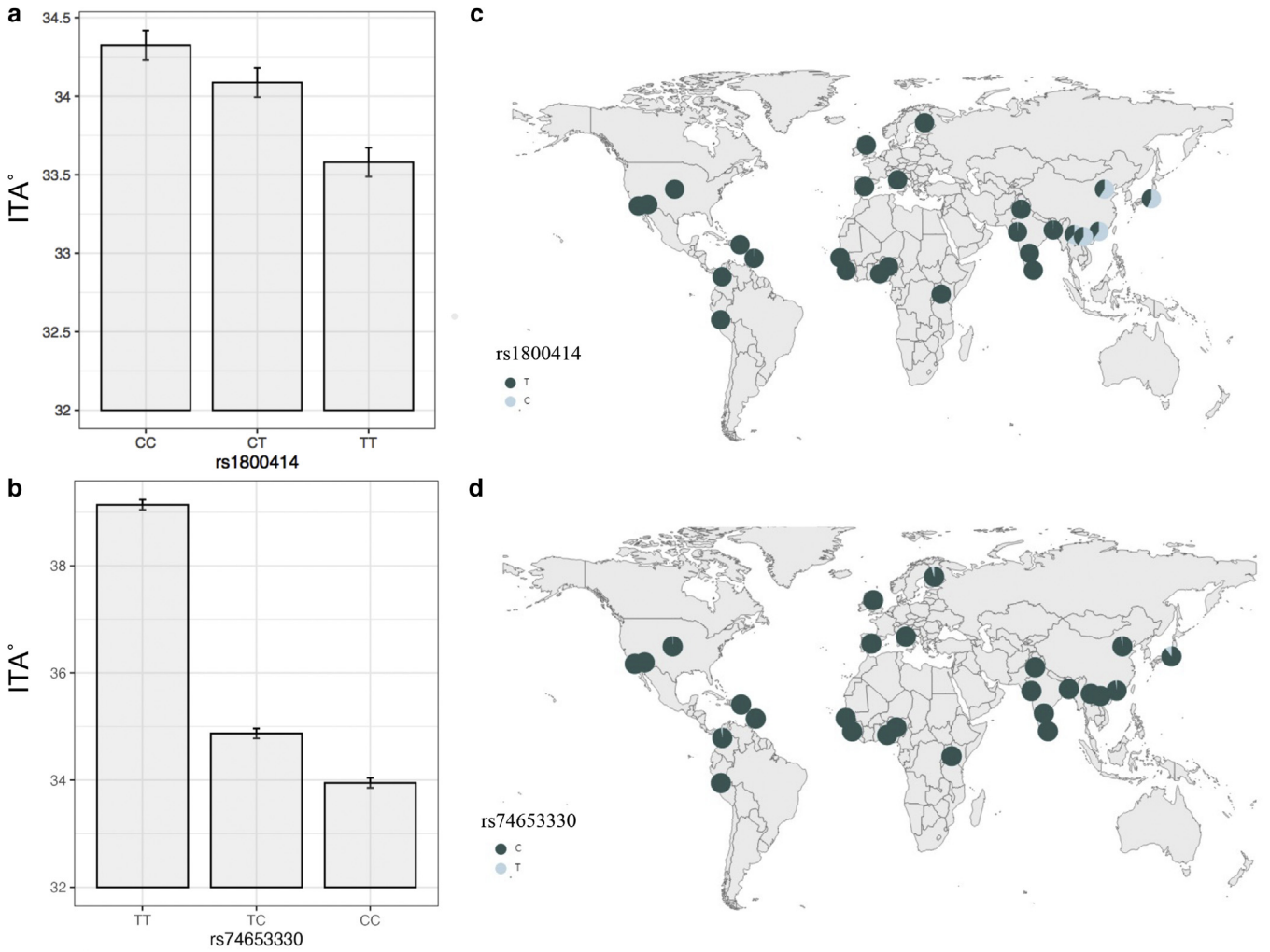

Supplementary Figure S5. Difference in skin color and allele frequencies. (**a**) The effect allele (C allele) of rs1800414 and (**b**) T allele of rs74653330 showed a lighting effect on skin color. Allele frequency data from 26 populations were taken from the 1000 Genome Project. For (**c**) rs1800414 and (**d**) rs74653330, ancestral alleles were represented in deep blue, derived alleles in water blue. ITA°, individual typology angle.

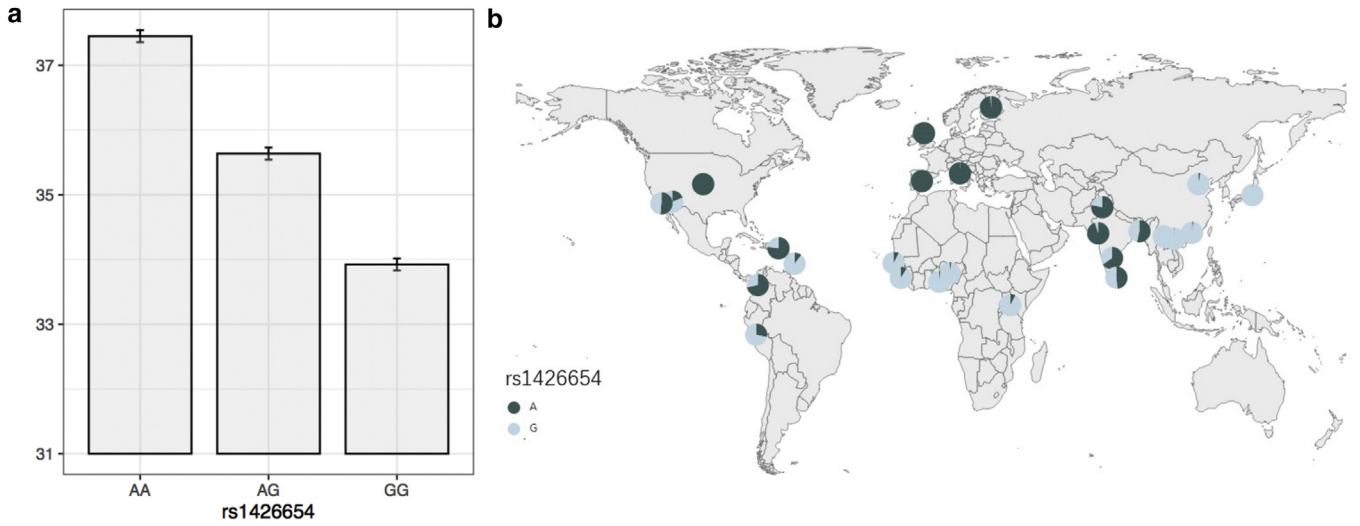

Supplementary Figure S6. Difference in skin color and allele frequencies of rs1426654. (**a**) The effect allele A of rs1426654 showed a lighting effect on skin color. (**b**) Geographical distribution of the allele frequencies for rs1426654.

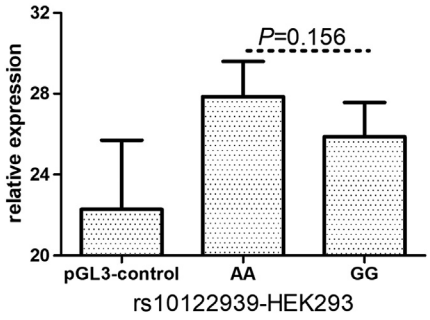

Supplementary Figure S7. Luciferase reporter assays in HEK293 cell line. The transcriptional activity of the enhancer containing the rs10122939 ancestral A allele was higher than that of the corresponding derived G allele in the HEK293 cell line.

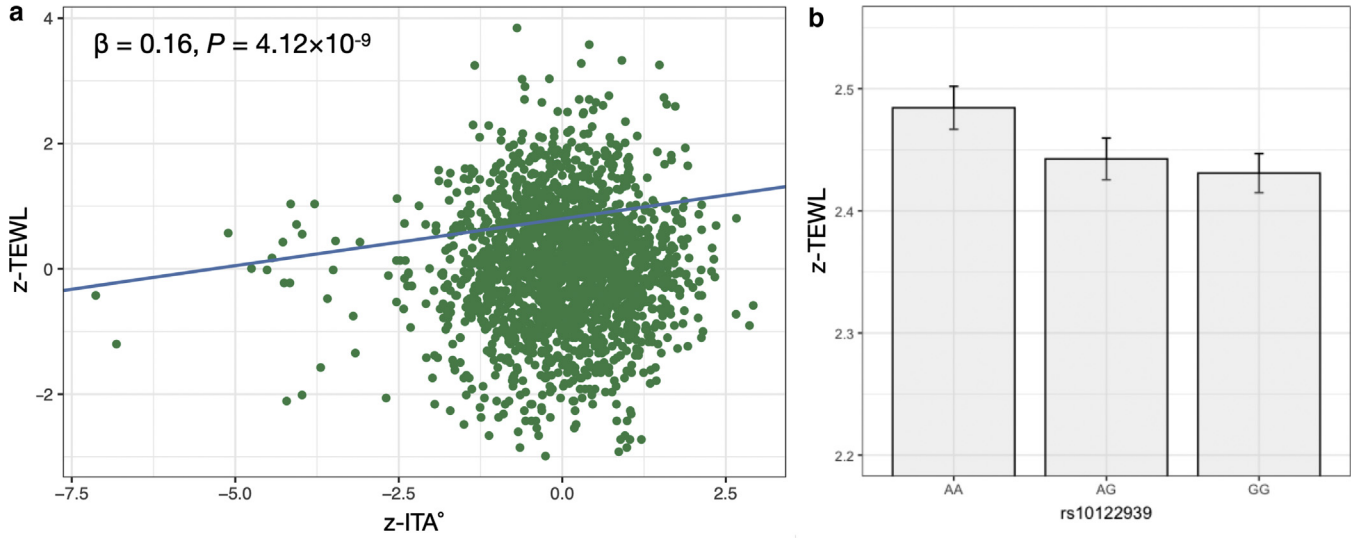

Supplementary Figure S8. The association analyses related to TEWL. (**a**) TEWL is positively associated with ITA° after controlling for age and sex, meaning better barrier function (thicker skin) s associated with darker skin. (**b**) ITA°-associated lead SNP rs10122939 was associated with TEWL. The darker skin (lower ITA°)–associated G allele has lower TEWL (thicker skin). ITA°, individual typology angle; TEWL, transepidermal water loss.

Supplementary Table S1. Sample Characteristics

Characteristic[1]	JD	NSPT	*P*[2]
Subjects, n	5,034	1,930	
Male sex, n (%)	2,501 (49.68)	705 (36.53)	7.09×10^{-23}
Age in y, median (IQR)	44.00(34.00–56.00)	51.00(40.00–58.00)	3.09×10^{-16}
ITA°, median (IQR)	36.59(32.42–40.89)	41.69(36.06–47.80)	1.31×10^{-151}
Skin color type, n (%)			
Very light (ITA° > 55°)	3 (0.06)	138 (7.15)	2.63×10^{-233}
Light (41° < ITA° < 55°)	1,214 (24.12)	897 (46.48)	
Intermediate (28° < ITA° < 41°)	3,439 (68.32)	804 (41.66)	
Tan (10° < ITA° < 28°)	378 (7.51)	73 (3.78)	
Brown (−30° < ITA° < 28°)	0 (0)	18 (0.93)	

Abbreviations: IQR, interquartile range; ITA°, individual topology angle; JD, Jidong cohort; NSPT, National Survey of Physical Traits cohort.
[1]Baseline characteristics were compared between the discovery dataset and the JD dataset.
[2]*P*-value of *t*-tests for continuous variables and χ^2 tests for categorical variables.

Supplementary Table S2. SNPs the Showing Genome-Wide Significant Association ($P < 5e{-}8$) with Skin Color ITA° in 6,964 Chinese Individuals

							JD (n = 5,034)				NSPT (n = 1,930)				META (n = 6,964)		EAF 1KGP		
SNP	Gene	CHR	MB	EA	OA	AA	EAF	Beta	SE	*P*	EAF	Beta	SE	*P*	Beta	P	EAS	EUR	AFR
rs10122939	*SLC24A2*	9	20.30	G	A	A	0.34	−0.10	0.02	1.29E−09	0.33	−0.07	0.02	4.71E−03	−0.09	3.61E−11	0.30	0.00	0.27
rs10116858	*SLC24A2*	9	20.30	T	G	T	0.34	−0.10	0.02	6.35E−09	0.32	−0.07	0.03	3.61E−03	−0.09	1.12E−10	0.30	0.00	0.24
rs10117511	*SLC24A2*	9	20.30	A	G	G	0.33	−0.10	0.02	5.03E−09	0.32	−0.07	0.03	3.65E−03	−0.09	9.34E−11	0.29	0.00	0.13
rs7033540	*SLC24A2*	9	20.30	T	C	C	0.29	−0.10	0.02	4.19E−08	0.28	−0.07	0.03	0.01	−0.09	2.21E−09	0.26	0.00	0.21
rs7037385	*SLC24A2*	9	20.30	A	G	G	0.30	−0.09	0.02	9.59E−08	0.28	−0.07	0.03	5.23E−03	−0.09	2.06E−09	0.27	0.00	0.26
rs12551950	*SLC24A2*	9	20.31	G	A	A	0.31	−0.09	0.02	6.37E−08	0.30	−0.08	0.03	2.62E−03	−0.09	6.62E−10	0.29	0.01	0.18
rs7851959	*SLC24A2*	9	20.31	C	G	G	0.31	−0.10	0.02	4.44E−08	0.30	−0.08	0.03	3.10E−03	−0.09	5.68E−10	0.71	0.99	0.62
rs58951095	*SLC24A2*	9	20.31	A	G	G	0.30	−0.09	0.02	8.63E−08	0.29	−0.08	0.03	2.74E−03	−0.09	9.29E−10	0.27	0.00	0.19
rs57500604	*SLC24A2*	9	20.31	A	C	C	0.30	−0.10	0.02	5.77E−08	0.29	−0.08	0.03	3.78E−03	−0.09	8.98E−10	0.27	0.01	0.31
rs16938009	*SLC24A2*	9	20.31	G	A	A	0.31	−0.09	0.02	6.54E−08	0.30	−0.08	0.03	2.87E−03	−0.09	7.54E−10	0.29	0.01	0.32
rs12555331	*SLC24A2*	9	20.31	G	C	C	0.30	−0.09	0.02	1.56E−07	0.29	−0.07	0.03	5.04E−03	−0.09	3.17E−09	0.73	1.00	0.81
rs1456966	*SLC24A2*	9	20.31	G	A	A	0.33	−0.08	0.02	2.37E−06	0.31	−0.07	0.03	5.23E−03	−0.08	4.27E−08	0.31	0.01	0.49
rs2383137	*SLC24A2*	9	20.32	C	G	G	0.32	−0.08	0.02	1.27E−06	0.30	−0.07	0.03	6.71E−03	−0.08	3.04E−08	0.70	0.99	0.82
rs7023559	*SLC24A2*	9	20.32	C	A	A	0.33	−0.08	0.02	2.00E−06	0.32	−0.07	0.03	5.02E−03	−0.08	3.48E−08	0.31	0.07	0.31
rs1800414	*OCA2*	15	28.19	T	C	T	0.48	−0.08	0.02	1.96E−06	0.46	−0.10	0.02	9.55E−06	−0.09	1.11E−10	0.40	1.00	1.00
rs76930569	*OCA2*	15	28.20	C	T	C	0.48	−0.08	0.02	1.96E−06	0.43	−0.10	0.02	9.55E−06	−0.09	1.11E−10	0.40	1.00	1.00
rs76470826	*OCA2*	15	28.22	AT	A	AT	0.48	−0.07	0.02	5.19E−06	0.43	−0.10	0.02	1.32E−05	−0.08	4.22E−10	0.59	0.00	0.00
rs74653330	*OCA2*	15	28.23	T	C	C	0.04	0.18	0.04	7.93E−06	0.02	0.21	0.06	9.88E−04	0.19	3.05E−08	0.03	0.01	0.00
rs1426654	*SLC24A5*	15	48.42	A	G	G	0.03	0.27	0.03	2.55E−09	0.03	0.16	0.03	3.00E−02	0.24	4.64E−10	0.01	1.00	0.07
rs2413887	*CTXN2*	15	48.49	C	T	T	0.04	0.22	0.04	2.93E−07	0.02	0.15	0.07	0.03	0.20	3.36E−08	0.02	1.00	0.08

Abbreviations: AA, ancestral allele; AFR, African; CHR, chromosome; EA, effect allele; EAF, effect allele frequency; EAS, East Asian; EUR, European; ITA°, individual topology angle; JD, Jidong cohort; NSPT, National Survey of Physical Traits cohort; OA, other allele; 1KGP, 1000 Genome Project.

Supplementary Table S3. SNPs Showing the Suggestive Association (5e−8 < *P* < 1e−6) with ITA° in the Meta-Analysis of 6,964 Chinese Individuals

							JD (n = 5,034)				NSPT (n = 1,930)				META (n = 6,964)		EAF 1KGP		
SNP	Gene	CHR	MB	EA	OA	AA	EAF	Beta	SE	*P*	EAF	Beta	SE	*P*	Beta	P	EAS	EUR	AFR
rs201197089	*GABBR1*	6	29.57	C	CT	CT	0.14	−0.10	0.02	1.08E−05	0.16	−0.08	0.04	0.02	−0.10	5.81E−07	0.30	0.00	0.27
rs11304792	*SLC24A2*	9	20.31	C	CT	CT	0.40	−0.07	0.02	8.16E−06	0.38	−0.07	0.02	5.02E−03	−0.07	1.34E−07	0.37	0.16	0.53
rs6475429	*SLC24A2*	9	20.31	C	A	C	0.47	−0.06	0.02	2.17E−04	0.43	−0.08	0.02	6.77E−04	−0.07	6.40E−07	0.41	0.50	0.94
rs28641053	*SLC24A2*	9	20.31	A	C	C	0.40	−0.07	0.02	1.85E−05	0.37	−0.08	0.02	9.09E−04	−0.07	6.15E−08	0.35	0.01	0.47
rs7021984	*SLC24A2*	9	20.31	A	T	T	0.33	−0.08	0.02	2.40E−06	0.31	−0.06	0.03	0.02	−0.08	1.47E−07	0.69	0.98	0.76
rs7023747	*SLC24A2*	9	20.32	T	G	T	0.34	−0.08	0.02	3.73E−06	0.34	−0.06	0.03	0.02	−0.07	3.05E−07	0.35	0.08	0.38
rs3915945	*RAB11FIP2*	10	119.75	A	G	G	0.15	0.10	0.02	4.03E−06	0.12	0.08	0.03	0.02	0.10	2.70E−07	0.13	0.01	0.00
rs116921893	*RAB11FIP2*	10	119.76	C	T	T	0.15	0.10	0.02	4.03E−06	0.12	0.08	0.03	0.02	0.10	2.70E−07	0.13	0.01	0.00
rs74638723	*RAB11FIP2*	10	119.77	G	A	A	0.15	0.10	0.02	5.03E−06	0.12	0.08	0.03	0.02	0.10	3.04E−07	0.13	0.01	0.01
rs3740550	*RAB11FIP2*	10	119.77	A	G	G	0.15	0.10	0.02	5.03E−06	0.12	0.08	0.03	0.02	0.10	3.04E−07	0.13	0.01	0.01
rs60424173	*RAB11FIP2*	10	119.78	G	T	T	0.16	0.10	0.02	9.13E−06	0.12	0.07	0.03	0.03	0.09	8.20E−07	0.13	0.01	0.01
rs79852633	*CASC2*	10	119.84	A	G	G	0.15	0.10	0.02	8.87E−06	0.12	0.10	0.03	3.28E−03	0.10	9.64E−08	0.13	0.01	0.00
rs79250499	*CASC2*	10	119.86	A	C	C	0.15	0.10	0.02	1.03E−05	0.12	0.10	0.03	4.22E−03	0.10	1.42E−07	0.13	0.01	0.01
rs7077320	*CASC2*	10	119.87	C	T	T	0.15	0.10	0.02	1.02E−05	0.11	0.10	0.03	3.23E−03	0.10	1.09E−07	0.13	0.01	0.01
rs61507658	*CASC2*	10	119.88	G	A	A	0.14	0.10	0.02	1.44E−05	0.10	0.11	0.04	1.67E−03	0.11	8.48E−08	0.11	0.01	0.00
rs201658840	*CASC2*	10	119.90	T	TG	TG	0.15	0.09	0.02	4.51E−05	0.12	0.10	0.03	3.15E−03	0.10	4.71E−07	0.13	0.01	0.01
rs75295597	*OCA2*	15	28.23	A	T	A	0.49	−0.06	0.02	1.88E−04	0.43	−0.09	0.02	6.76E−05	−0.07	8.67E−08	0.39	1.00	1.00
rs12442916	*OCA2*	15	28.23	G	A	G	0.37	−0.06	0.02	2.81E−04	0.35	−0.09	0.02	1.82E−04	−0.07	3.00E−07	0.30	0.94	1.00
rs10775262	*OCA2*	15	28.23	T	C	C	0.36	−0.06	0.02	6.46E−04	0.34	−0.09	0.02	2.37E−04	−0.07	9.21E−07	0.29	0.87	0.80
rs10775263	*OCA2*	15	28.23	C	T	C	0.36	−0.06	0.02	6.46E−04	0.34	−0.09	0.02	2.37E−04	−0.07	9.21E−07	0.29	0.87	0.80
rs730502	*OCA2*	15	28.23	G	T	G	0.36	−0.06	0.02	5.01E−04	0.34	−0.09	0.02	1.70E−04	−0.07	5.39E−07	0.29	0.87	0.80
rs2267434	*ACO2*	22	41.88	T	C	C	0.41	0.07	0.02	1.79E−05	0.51	0.06	0.02	0.01	0.07	8.59E−07	0.51	0.01	0.26
rs5751114	*ACO2*	22	41.88	G	A	G	0.41	0.07	0.02	1.24E−05	0.51	0.06	0.02	0.02	0.07	7.27E−07	0.51	0.02	0.52
rs2267435	*ACO2*	22	41.88	G	A	A	0.41	0.07	0.02	1.85E−05	0.51	0.06	0.02	0.01	0.07	8.83E−07	0.51	0.01	0.21
rs2284080	*ACO2*	22	41.89	C	G	G	0.41	0.07	0.02	1.85E−05	0.51	0.06	0.02	0.01	0.07	8.83E−07	0.49	0.99	0.79
rs5751123	*POLR3H*	22	41.93	A	C	C	0.42	0.07	0.02	2.83E−05	0.52	0.06	0.02	9.28E−03	0.07	8.36E−07	0.52	0.01	0.22
rs5758384	*POLR3H*	22	41.93	T	G	G	0.42	0.07	0.02	2.83E−05	0.52	0.06	0.02	9.28E−03	0.07	8.36E−07	0.52	0.01	0.22
rs5758386	*POLR3H*	22	41.94	A	G	G	0.42	0.07	0.02	3.01E−05	0.52	0.06	0.02	9.82E−03	0.07	9.42E−07	0.52	0.01	0.57
rs5758388	*POLR3H*	22	41.94	T	C	C	0.42	0.07	0.02	2.83E−05	0.52	0.06	0.02	9.28E−03	0.07	8.36E−07	0.52	0.01	0.22
rs8138232	*POLR3H*	22	41.94	T	C	C	0.42	0.07	0.02	2.83E−05	0.52	0.06	0.02	9.28E−03	0.07	8.36E−07	0.52	0.01	0.23

Abbreviations: AA, ancestral allele; AFR, African; CHR, chromosome; EA, effect allele; EAF, effect allele frequency; EAS, East Asian; EUR, European; ITA°, individual topology angle; JD, Jidong cohort; NSPT, National Survey of Physical Traits cohort; OA: other allele; 1KGP: 1000 Genome Project.

Table S4. Replication of a Total of 9,183 SNPs Associated with Skin Tanning, Skin Pigmentation, Hair Color, and Eye Color From Visconti et al., Adhikari et al., Hysi et al., and Simcoe et al. in META Results

						JD (N = 5,034)				NSPT (N = 1,930)				META (N = 6,964)		EAF			
SNP	Gene	CHR	MB	EA	OA	EAF	Beta	SE	*P*	EAF	Beta	SE	*P*	Beta	*P*	EAS	EUR	AFR	Related Trait
rs1426654	*SLC24A5*	15	48.43	G	A	0.97	0.27	0.05	2.55E−09	0.98	0.16	0.07	2.71E−02	0.24	4.64E−10	0.99	0.00	0.93	Skin, hair and eye color; skin tanning
rs2413887	*SLC24A5*	15	48.49	T	C	0.96	0.22	0.04	2.93E−07	0.98	0.15	0.07	2.70E−02	0.20	3.36E−08	0.98	0.00	0.92	Skin tanning
rs12442916	*OCA2*	15	28.23	A	G	0.63	−0.06	0.02	2.81E−04	0.65	−0.09	0.02	1.82E−04	−0.07	3.00E−07	0.70	0.06	0.00	Skin tanning
rs730502	*OCA2*	15	28.23	T	G	0.64	−0.06	0.02	5.01E−04	0.66	−0.09	0.02	1.70E−04	−0.07	5.39E−07	0.71	0.13	0.20	Skin tanning
rs10775262	*OCA2*	15	28.23	C	T	0.64	−0.06	0.02	6.46E−04	0.66	−0.09	0.02	2.37E−04	−0.07	9.21E−07	0.71	0.13	0.20	Skin tanning
rs10775263	*OCA2*	15	28.23	T	C	0.64	−0.06	0.02	6.46E−04	0.66	−0.09	0.02	2.37E−04	−0.07	9.21E−07	0.71	0.13	0.20	Skin tanning
rs12438490	*OCA2*	15	28.26	T	C	0.60	−0.04	0.02	1.11E−02	0.67	−0.08	0.02	7.67E−04	−0.05	6.36E−05	0.69	0.03	0.06	Skin tanning
rs113769342	*DEF8*	16	89.98	T	C	0.06	0.15	0.03	1.21E−05	0.05	0.03	0.05	5.85E−01	0.11	8.41E−05	0.04	0.01	0.00	Skin tanning
rs112597872	*DEF8*	16	89.97	C	G	0.06	0.17	0.04	3.49E−06	0.04	0.00	0.05	9.94E−01	0.11	1.21E−04	0.96	0.99	1.00	Skin tanning
rs4778136	*OCA2*	15	28.25	C	T	0.54	−0.04	0.02	2.80E−02	0.59	−0.08	0.02	7.28E−04	−0.05	1.86E−04	0.62	0.10	0.38	Skin tanning
rs1800404	*OCA2*	15	28.24	T	C	0.00	0.04	0.02	2.00E−02	0.00	0.07	0.02	1.60E−03	−0.05	2.08E−04	0.42	0.79	0.12	Skin color
rs12440330	*OCA2*	15	28.25	T	C	0.52	−0.04	0.02	1.95E−02	0.58	−0.07	0.02	1.88E−03	−0.05	2.20E−04	0.61	0.03	0.01	Skin tanning
rs116848174	*FANCA*	16	89.90	T	A	0.06	0.16	0.04	6.62E−06	0.04	−0.01	0.05	8.65E−01	0.11	2.73E−04	0.95	0.99	1.00	Skin tanning
rs4778224	*OCA2*	15	28.24	G	A	0.00	−0.04	0.02	2.93E−02	0.44	−0.07	0.02	1.89E−03	−0.05	3.62E−04	0.39	0.85	0.47	Eye color
rs1868333	*OCA2*	15	28.24	A	G	0.00	−0.04	0.02	2.49E−02	0.43	−0.07	0.02	2.67E−03	−0.05	3.70E−04	0.39	0.79	0.13	Eye color
rs735066	*OCA2*	15	28.24	G	A	0.00	−0.04	0.02	2.49E−02	0.43	−0.07	0.02	2.67E−03	−0.05	3.70E−04	0.39	0.79	0.13	Eye color
rs11630828	*OCA2*	15	28.24	A	G	0.00	−0.04	0.02	2.77E−02	0.43	−0.07	0.02	2.67E−03	−0.05	4.22E−04	0.39	0.79	0.21	Eye color
rs7178315	*OCA2*	15	28.24	C	T	0.00	−0.04	0.02	2.77E−02	0.43	−0.07	0.02	2.67E−03	−0.05	4.22E−04	0.39	0.78	0.21	Eye color
rs1868332	*OCA2*	15	28.24	A	G	0.00	−0.04	0.02	2.77E−02	0.43	−0.07	0.02	2.67E−03	−0.05	4.22E−04	0.38	0.79	0.21	Eye color
rs1868334	*OCA2*	15	28.24	A	C	0.00	−0.04	0.02	2.77E−02	0.43	−0.07	0.02	2.67E−03	−0.05	4.22E−04	0.39	0.79	0.21	Eye color
rs12595216	*OCA2*	15	28.24	G	A	0.00	−0.04	0.02	2.77E−02	0.43	−0.07	0.02	2.67E−03	−0.05	4.22E−04	0.39	0.79	0.21	Eye color
rs136402	*EP300*	22	41.60	A	G	0.31	0.06	0.02	1.32E−03	0.38	0.04	0.02	1.01E−01	0.05	4.52E−04	0.41	0.31	0.38	Hair color
rs112225320	*VPS9D1*	16	89.85	C	A	0.06	0.14	0.03	3.34E−05	0.04	0.00	0.05	9.28E−01	0.10	4.89E−04	0.05	0.01	0.00	Skin tanning
rs113234026	*ZNF276*	16	89.88	G	A	0.06	0.16	0.04	7.93E−06	0.04	−0.02	0.05	6.75E−01	0.10	5.52E−04	0.05	0.01	0.00	Skin tanning
rs2302161	*SPATA2L*	16	89.85	T	C	0.06	0.14	0.03	6.09E−05	0.04	0.01	0.05	9.07E−01	0.10	7.30E−04	0.04	0.01	0.00	Skin tanning
rs4778219	*OCA2*	15	28.21	C	T	0.00	0.05	0.02	2.10E−02	0.00	0.08	0.03	1.11E−02	−0.06	8.16E−04	0.12	0.87	0.81	Skin color
rs8035315	*OCA2*	15	28.21	T	G	0.00	−0.05	0.02	2.12E−02	0.16	−0.08	0.03	1.42E−02	−0.06	9.72E−04	0.16	0.67	0.11	Eye color
rs7349397	*PRKCE*	2	46.25	T	C	0.00	0.07	0.02	3.67E−03	0.13	0.05	0.04	1.55E−01	0.06	1.36E−03	0.14	0.25	0.37	Eye color
rs7274168	*ZNF341*	20	32.44	T	C	0.90	−0.07	0.03	1.24E−02	0.91	−0.09	0.04	4.58E−02	−0.07	1.45E−03	0.90	0.54	0.37	Skin tanning
rs1810534	*ZNF341*	20	32.44	T	C	0.90	−0.07	0.03	1.38E−02	0.91	−0.09	0.04	4.48E−02	−0.07	1.60E−03	0.90	0.54	0.36	Skin tanning
rs13041078	*ZNF341*	20	32.44	T	G	0.90	−0.07	0.03	1.18E−02	0.91	−0.08	0.04	5.67E−02	−0.07	1.63E−03	0.90	0.51	0.34	Skin tanning
rs75092208	*SPATA33*	16	89.81	C	T	0.07	0.10	0.03	1.22E−03	0.06	0.03	0.05	4.72E−01	0.08	2.02E−03	0.05	0.01	0.00	Skin tanning
rs535070	*PIEZO1*	16	88.88	G	A	0.74	−0.06	0.02	2.56E−03	0.69	−0.03	0.03	2.82E−01	−0.05	2.03E−03	0.69	0.36	0.80	Skin tanning
rs2788222	*EXOC2*	6	0.72	G	T	0.11	−0.08	0.03	4.42E−03	0.10	−0.05	0.04	1.89E−01	−0.07	2.04E−03	0.13	0.34	0.58	Skin tanning
rs530782	*GRM5*	11	88.57	G	T	0.59	0.06	0.02	3.03E−04	0.60	0.00	0.02	8.83E−01	0.04	2.23E−03	0.62	0.28	0.79	Skin tanning
rs112992887	*VPS9D1*	16	89.86	A	G	0.07	0.13	0.03	6.80E−05	0.05	−0.02	0.05	6.59E−01	0.08	2.24E−03	0.05	0.01	0.00	Skin tanning
rs2804737	*EXOC2*	6	0.72	G	A	0.11	−0.07	0.03	5.50E−03	0.10	−0.05	0.04	1.75E−01	−0.07	2.27E−03	0.13	0.34	0.70	Skin tanning
rs7928319	*TPCN2*	11	68.91	A	G	0.15	−0.05	0.02	2.50E−02	0.13	−0.07	0.03	3.44E−02	−0.06	2.33E−03	0.11	0.30	0.23	Skin tanning
rs6120392	*ZNF341*	20	32.45	A	G	0.91	−0.07	0.03	1.06E−02	0.92	−0.07	0.04	1.05E−01	−0.07	2.46E−03	0.91	0.51	0.84	Skin tanning

(*continued*)

Table S4. Continued

						JD (N = 5,034)				NSPT (N = 1,930)				META (N = 6,964)		EAF			
SNP	Gene	CHR	MB	EA	OA	EAF	Beta	SE	*P*	EAF	Beta	SE	*P*	Beta	*P*	EAS	EUR	AFR	Related Trait
rs57995073	*ZNF341*	20	32.45	A	C	0.91	−0.07	0.03	1.06E−02	0.92	−0.07	0.04	1.05E−01	−0.07	2.46E−03	0.91	0.51	0.90	Skin tanning
rs4911133	*ZNF341*	20	32.45	A	G	0.91	−0.07	0.03	1.06E−02	0.92	−0.07	0.04	1.05E−01	−0.07	2.46E−03	0.91	0.51	0.90	Skin tanning
rs6059501	*ZNF341*	20	32.45	A	T	0.91	−0.07	0.03	1.06E−02	0.92	−0.07	0.04	1.05E−01	−0.07	2.46E−03	0.09	0.49	0.19	Skin tanning
rs4961760	*BNC2*	9	16.79	C	T	0.12	−0.08	0.03	1.10E−03	0.13	−0.02	0.03	5.20E−01	−0.06	2.56E−03	0.12	0.06	0.20	Skin tanning
rs6059496	*ZNF341*	20	32.45	C	T	0.91	−0.07	0.03	1.14E−02	0.92	−0.07	0.04	1.03E−01	−0.07	2.61E−03	0.91	0.50	0.84	Skin tanning
rs6059497	*ZNF341*	20	32.45	G	C	0.91	−0.07	0.03	1.14E−02	0.92	−0.07	0.04	1.03E−01	−0.07	2.61E−03	0.09	0.49	0.16	Skin tanning
rs116953717	*CDK10*	16	89.83	G	A	0.08	0.11	0.03	2.72E−04	0.07	0.00	0.04	9.91E−01	0.07	2.62E−03	0.06	0.01	0.00	Skin tanning
rs555464	*GRM5*	11	88.57	T	A	0.59	0.06	0.02	3.16E−04	0.60	0.00	0.02	9.60E−01	0.04	2.75E−03	0.38	0.72	0.22	Skin tanning
rs6059498	*ZNF341*	20	32.45	C	T	0.91	−0.07	0.03	1.18E−02	0.92	−0.07	0.04	1.11E−01	−0.07	2.88E−03	0.91	0.51	0.84	Skin tanning
rs6059499	*ZNF341*	20	32.45	C	T	0.91	−0.07	0.03	1.18E−02	0.92	−0.07	0.04	1.11E−01	−0.07	2.88E−03	0.91	0.51	0.84	Skin tanning
rs530975	*GRM5*	11	88.57	T	C	0.59	0.06	0.02	3.35E−04	0.60	0.00	0.02	9.79E−01	0.04	2.98E−03	0.62	0.28	0.66	Skin tanning
rs2378024	*ZNF341*	20	32.44	G	C	0.90	−0.07	0.03	1.35E−02	0.92	−0.07	0.04	1.00E−01	−0.07	2.99E−03	0.09	0.49	0.61	Skin tanning
rs79361800	*MIR200B*	1	1.18	C	G	0.25	−0.04	0.02	2.00E−02	0.24	−0.05	0.03	8.17E−02	−0.05	3.07E−03	0.17	0.09	0.15	Hair color
rs2293585	*FANCA*	16	89.89	T	C	0.07	0.13	0.03	2.75E−05	0.05	−0.04	0.05	3.59E−01	0.08	3.07E−03	0.06	0.01	0.00	Skin tanning
rs117555146	*CDK10*	16	89.83	T	C	0.08	0.11	0.03	3.48E−04	0.07	0.00	0.04	9.96E−01	0.07	3.12E−03	0.06	0.01	0.00	Skin tanning
rs11021369	*GRM5*	11	88.54	C	G	0.59	0.06	0.02	4.89E−04	0.60	0.00	0.02	9.24E−01	0.04	3.43E−03	0.38	0.77	0.24	Skin tanning
rs118066878	*SPG7*	16	89.65	A	G	0.11	0.04	0.03	9.10E−02	0.12	0.10	0.04	7.49E−03	0.06	3.70E−03	0.13	0.10	0.00	Skin tanning
rs6120395	*ZNF341*	20	32.45	G	A	0.91	−0.07	0.03	1.59E−02	0.92	−0.07	0.04	1.13E−01	−0.07	3.90E−03	0.91	0.51	0.97	Skin tanning
rs2788224	*EXOC2*	6	0.72	G	A	0.10	−0.07	0.03	6.30E−03	0.10	−0.04	0.04	2.71E−01	−0.06	4.12E−03	0.13	0.34	0.57	Skin tanning
rs6088301	*PXMP4*	20	32.37	C	A	0.38	0.03	0.02	8.66E−02	0.36	0.06	0.02	1.02E−02	0.04	4.24E−03	0.32	0.34	0.24	Skin tanning
rs17226764	*CDK10*	16	89.83	G	GAC	0.08	0.10	0.03	8.50E−04	0.07	0.01	0.04	8.67E−01	0.07	4.25E−03	0.06	0.01	0.00	Skin tanning
rs2804738	*EXOC2*	6	0.73	G	A	0.10	−0.07	0.03	8.41E−03	0.10	−0.05	0.04	2.28E−01	−0.06	4.39E−03	0.13	0.34	0.40	Skin tanning
rs2804739	*EXOC2*	6	0.73	G	A	0.10	−0.07	0.03	8.41E−03	0.10	−0.05	0.04	2.28E−01	−0.06	4.39E−03	0.13	0.34	0.40	Skin tanning
rs6088300	*PXMP4*	20	32.37	C	T	0.38	0.03	0.02	8.11E−02	0.36	0.06	0.02	1.27E−02	0.04	4.48E−03	0.32	0.34	0.25	Skin tanning
rs7187583	*ACSF3*	16	89.17	G	A	0.68	−0.04	0.02	2.05E−02	0.71	−0.04	0.03	1.03E−01	−0.04	4.61E−03	0.68	0.29	0.47	Skin tanning
rs12221717	*GRM5*	11	88.54	T	G	0.59	0.06	0.02	6.77E−04	0.60	0.00	0.02	9.69E−01	0.04	4.83E−03	0.61	0.28	0.76	Skin tanning
rs6059462	*PXMP4*	20	32.36	T	C	0.38	0.03	0.02	8.26E−02	0.36	0.06	0.02	1.42E−02	0.04	4.92E−03	0.32	0.34	0.27	Skin tanning
rs7202996	*ACSF3*	16	89.17	G	A	0.68	−0.04	0.02	2.01E−02	0.71	−0.04	0.03	1.20E−01	−0.04	5.13E−03	0.68	0.30	0.47	Skin tanning
rs736953	*ZNF341*	20	32.42	T	G	0.90	−0.06	0.03	2.41E−02	0.91	−0.07	0.04	9.91E−02	−0.06	5.29E−03	0.90	0.50	0.36	Skin tanning
rs11478076	*PXMP4*	20	32.38	C	CT	0.38	0.03	0.02	1.17E−01	0.36	0.06	0.02	7.73E−03	0.04	5.29E−03	0.32	0.34	0.32	Skin tanning
rs7202765	*ACSF3*	16	89.17	G	A	0.68	−0.04	0.02	2.08E−02	0.71	−0.04	0.03	1.20E−01	−0.04	5.30E−03	0.68	0.30	0.42	Skin tanning
rs2626558	*ZNF341*	20	32.43	A	G	0.91	−0.07	0.03	1.64E−02	0.92	−0.06	0.04	1.63E−01	−0.07	5.52E−03	0.90	0.51	0.71	Skin tanning
rs10741523	*GRM5*	11	88.52	C	T	0.59	0.05	0.02	1.06E−03	0.60	0.00	0.02	9.04E−01	0.04	5.77E−03	0.62	0.28	0.72	Skin tanning
rs319032	*NOX4*	11	89.17	T	G	0.54	0.04	0.02	2.67E−02	0.53	0.04	0.02	1.00E−01	0.04	5.82E−03	0.53	0.35	0.52	Skin tanning
rs2103804	*ZNF341*	20	32.43	T	C	0.90	−0.06	0.03	2.41E−02	0.92	−0.07	0.04	1.17E−01	−0.06	6.06E−03	0.90	0.51	0.37	Skin tanning
rs11493150	*GRM5*	11	88.61	T	C	0.07	0.11	0.03	5.21E−04	0.07	0.00	0.04	9.30E−01	0.07	6.19E−03	0.05	0.02	0.01	Skin tanning
rs2788219	*EXOC2*	6	0.71	C	T	0.08	−0.07	0.03	1.81E−02	0.08	−0.06	0.04	1.63E−01	−0.07	6.22E−03	0.10	0.23	0.47	Skin tanning
rs35965351	*PXMP4*	20	32.37	A	AC	0.38	0.03	0.02	1.04E−01	0.35	0.06	0.02	1.33E−02	0.04	6.24E−03	0.31	0.34	0.31	Skin tanning
rs4105582	*GRM5*	11	88.53	C	A	0.59	0.05	0.02	1.16E−03	0.60	0.00	0.02	9.21E−01	0.04	6.39E−03	0.62	0.28	0.67	Skin tanning
rs11908486	*MANBAL*	20	35.98	T	G	0.03	−0.09	0.05	7.49E−02	0.02	−0.18	0.08	2.35E−02	−0.12	6.55E−03	0.01	0.21	0.39	Skin tanning
rs2092737	*ZNF341*	20	32.43	C	A	0.91	−0.06	0.03	2.59E−02	0.92	−0.07	0.04	1.19E−01	−0.06	6.58E−03	0.91	0.51	0.37	Skin tanning

Table S4. Continued

						JD (N = 5,034)				NSPT (N = 1,930)				META (N = 6,964)		EAF			
SNP	Gene	CHR	MB	EA	OA	EAF	Beta	SE	*P*	EAF	Beta	SE	*P*	Beta	*P*	EAS	EUR	AFR	Related Trait
rs12419811	*GRM5*	11	88.53	A	G	0.14	0.07	0.02	2.65E−03	0.13	0.01	0.03	6.76E−01	0.05	6.64E−03	0.10	0.03	0.05	Skin tanning
rs10756846	*BNC2*	9	16.95	G	C	0.08	0.05	0.03	8.00E−02	0.07	0.10	0.05	2.19E−02	0.07	6.70E−03	0.10	0.17	0.38	Skin tanning
rs11021556	*GRM5*	11	88.57	T	C	0.07	0.11	0.03	4.89E−04	0.07	−0.01	0.04	8.58E−01	0.07	6.89E−03	0.05	0.02	0.01	Skin tanning
rs1903841	*GRM5*	11	88.53	T	C	0.59	0.05	0.02	1.32E−03	0.60	0.00	0.02	9.23E−01	0.04	7.01E−03	0.62	0.28	0.77	Skin tanning
rs117941243	*GRM5*	11	88.60	A	G	0.07	0.11	0.03	5.21E−04	0.07	−0.01	0.04	8.69E−01	0.07	7.14E−03	0.05	0.02	0.01	Skin tanning
rs13006518	*PRKCE*	2	46.22	T	C	0.00	0.05	0.02	2.54E−02	0.13	0.05	0.04	1.41E−01	0.05	7.45E−03	0.14	0.23	0.30	Eye color
rs2804740	*EXOC2*	6	0.73	A	G	0.11	−0.07	0.03	1.23E−02	0.10	−0.04	0.04	2.76E−01	−0.06	7.47E−03	0.13	0.34	0.68	Skin tanning
rs1304320	*NOX4*	11	89.18	T	G	0.53	0.03	0.02	3.45E−02	0.52	0.04	0.02	1.02E−01	0.04	7.56E−03	0.53	0.43	0.27	Skin tanning
rs164741	*SPG7*	16	89.69	A	G	0.91	−0.10	0.03	5.45E−04	0.93	0.02	0.04	6.53E−01	−0.06	7.66E−03	0.93	0.34	0.40	Skin tanning
rs2747560	*PXMP4*	20	32.36	G	A	0.39	0.03	0.02	1.24E−01	0.37	0.06	0.02	1.32E−02	0.04	7.74E−03	0.34	0.34	0.74	Skin tanning
rs35732924	*MANBAL*	20	35.98	C	G	0.03	−0.08	0.05	8.93E−02	0.02	−0.18	0.08	2.19E−02	−0.11	7.77E−03	0.99	0.78	0.58	Skin tanning
rs2889785	*PXMP4*	20	32.37	C	T	0.39	0.02	0.02	1.32E−01	0.37	0.06	0.02	1.22E−02	0.04	7.96E−03	0.33	0.34	0.74	Skin tanning
rs11478671	*ZNF341*	20	32.41	T	TA	0.91	−0.07	0.03	1.64E−02	0.92	−0.05	0.04	2.45E−01	−0.06	8.04E−03	0.90	0.50	0.70	Skin tanning
rs4002398	*GRM5*	11	88.53	T	C	0.59	0.05	0.02	1.58E−03	0.60	0.00	0.02	9.31E−01	0.04	8.10E−03	0.62	0.28	0.77	Skin tanning
rs171307	*ANKRD11*	16	89.64	C	T	0.11	0.04	0.03	1.43E−01	0.11	0.10	0.04	1.09E−02	0.06	8.11E−03	0.11	0.08	0.01	Skin tanning
rs72643352	*NOX4*	11	89.39	C	T	0.22	0.06	0.02	1.20E−03	0.21	0.00	0.03	9.94E−01	0.04	8.14E−03	0.19	0.08	0.00	Skin tanning
rs1808431	*ANKRD11*	16	89.42	A	G	0.11	0.05	0.03	6.10E−02	0.10	0.07	0.04	5.16E−02	0.06	8.16E−03	0.12	0.07	0.00	Skin tanning
rs992702	*GRM5*	11	88.54	C	A	0.46	−0.05	0.02	1.50E−03	0.49	0.00	0.02	9.67E−01	−0.03	8.21E−03	0.52	0.25	0.40	Skin tanning
rs11021647	*GRM5*	11	88.61	T	C	0.07	0.11	0.03	6.91E−04	0.07	−0.01	0.04	8.78E−01	0.07	8.27E−03	0.05	0.02	0.01	Skin tanning
rs187794284	*GRM5*	11	88.62	C	T	0.07	0.11	0.03	6.17E−04	0.07	−0.01	0.04	8.55E−01	0.07	8.29E−03	0.05	0.02	0.02	Skin tanning
rs139861745	*GRM5*	11	88.62	C	T	0.07	0.11	0.03	6.17E−04	0.07	−0.01	0.04	8.55E−01	0.07	8.29E−03	0.05	0.02	0.02	Skin tanning
rs118099397	*GRM5*	11	88.62	A	C	0.07	0.11	0.03	6.17E−04	0.07	−0.01	0.04	8.55E−01	0.07	8.29E−03	0.05	0.02	0.02	Skin tanning
rs12363229	*GRM5*	11	88.62	T	C	0.07	0.11	0.03	6.17E−04	0.07	−0.01	0.04	8.55E−01	0.07	8.29E−03	0.05	0.02	0.02	Skin tanning
rs4911363	*PXMP4*	20	32.37	G	A	0.39	0.03	0.02	1.25E−01	0.37	0.06	0.02	1.49E−02	0.04	8.36E−03	0.33	0.34	0.47	Skin tanning
rs4911132	*PXMP4*	20	32.37	G	A	0.39	0.02	0.02	1.34E−01	0.37	0.06	0.02	1.28E−02	0.04	8.36E−03	0.33	0.34	0.73	Skin tanning
rs10810694	*BNC2*	9	16.95	C	G	0.08	0.05	0.03	8.63E−02	0.07	0.10	0.05	2.69E−02	0.06	8.40E−03	0.10	0.16	0.31	Skin tanning
rs10765809	*GRM5*	11	88.59	T	A	0.07	0.11	0.03	5.76E−04	0.07	−0.01	0.04	8.18E−01	0.07	8.41E−03	0.95	0.98	0.85	Skin tanning
rs1391954	*GRM5*	11	88.58	T	G	0.60	−0.05	0.02	3.35E−03	0.56	−0.01	0.02	7.13E−01	−0.04	8.49E−03	0.54	0.43	0.53	Skin tanning
rs4270425	*PXMP4*	20	32.37	A	G	0.39	0.02	0.02	1.45E−01	0.37	0.06	0.02	1.11E−02	0.04	8.51E−03	0.33	0.34	0.45	Skin tanning
rs6087519	*PXMP4*	20	32.36	C	G	0.39	0.03	0.02	1.24E−01	0.37	0.06	0.02	1.59E−02	0.04	8.59E−03	0.67	0.66	0.18	Skin tanning
rs7271022	*PXMP4*	20	32.37	C	T	0.39	0.03	0.02	1.24E−01	0.37	0.06	0.02	1.59E−02	0.04	8.59E−03	0.33	0.34	0.84	Skin tanning
rs2747562	*PXMP4*	20	32.38	T	C	0.37	0.03	0.02	9.21E−02	0.35	0.05	0.02	2.84E−02	0.04	8.65E−03	0.31	0.34	0.74	Skin tanning
rs79743671	*OCA2*	15	28.32	A	G	0.60	−0.02	0.02	1.42E−01	0.64	−0.06	0.02	1.28E−02	−0.04	8.65E−03	0.63	0.08	0.06	Skin tanning
rs2626522	*ZNF341*	20	32.40	G	C	0.90	−0.06	0.03	2.87E−02	0.92	−0.06	0.04	1.47E−01	−0.06	8.67E−03	0.10	0.49	0.65	Skin tanning
rs2243719	*BNC2*	9	16.81	T	A	0.09	−0.07	0.03	8.68E−03	0.15	−0.03	0.04	3.77E−01	−0.06	8.71E−03	0.84	0.94	0.84	Skin tanning
rs28469723	*TRPC4AP*	20	33.70	G	A	0.07	0.04	0.03	2.67E−01	0.09	0.13	0.04	3.37E−03	0.07	8.74E−03	0.09	0.09	0.17	Skin tanning
rs79341738	*TRPC4AP*	20	33.70	C	T	0.07	0.04	0.03	2.67E−01	0.09	0.13	0.04	3.37E−03	0.07	8.74E−03	0.09	0.09	0.16	Skin tanning
rs79438986	*TRPC4AP*	20	33.70	G	T	0.07	0.04	0.03	2.67E−01	0.09	0.13	0.04	3.37E−03	0.07	8.74E−03	0.09	0.09	0.05	Skin tanning
rs112318873	*TRPC4AP*	20	33.70	C	T	0.07	0.04	0.03	2.67E−01	0.09	0.13	0.04	3.37E−03	0.07	8.74E−03	0.09	0.09	0.17	Skin tanning
rs75888794	*TRPC4AP*	20	33.70	C	G	0.07	0.04	0.03	2.67E−01	0.09	0.13	0.04	3.37E−03	0.07	8.74E−03	0.91	0.91	0.83	Skin tanning
rs144862523	*GRM5*	11	88.62	A	G	0.07	0.11	0.03	6.76E−04	0.07	−0.01	0.04	8.55E−01	0.07	8.77E−03	0.05	0.02	0.02	Skin tanning

(*continued*)

Table S4. Continued

						JD (N = 5,034)				NSPT (N = 1,930)				META (N = 6,964)		EAF			
SNP	Gene	CHR	MB	EA	OA	EAF	Beta	SE	*P*	EAF	Beta	SE	*P*	Beta	*P*	EAS	EUR	AFR	Related Trait
rs13043800	*PXMP4*	20	32.37	C	T	0.39	0.02	0.02	1.30E−01	0.37	0.06	0.02	1.49E−02	0.04	8.80E−03	0.33	0.34	0.83	Skin tanning
rs112380351	*OCA2*	15	28.32	G	C	0.60	−0.02	0.02	1.46E−01	0.64	−0.06	0.02	1.28E−02	−0.04	8.94E−03	0.37	0.92	0.93	Skin tanning
rs10831459	*GRM5*	11	88.54	A	G	0.52	0.05	0.02	2.23E−03	0.53	0.00	0.02	8.71E−01	0.03	9.10E−03	0.55	0.28	0.63	Skin tanning
rs585423	*GRM5*	11	88.63	C	G	0.31	0.05	0.02	1.91E−03	0.30	0.00	0.03	9.37E−01	0.04	9.12E−03	0.71	0.62	0.71	Skin tanning
rs10765802	*GRM5*	11	88.57	T	C	0.07	0.11	0.03	6.49E−04	0.07	−0.01	0.04	8.06E−01	0.07	9.16E−03	0.05	0.02	0.00	Skin tanning
rs10765803	*GRM5*	11	88.57	T	C	0.07	0.11	0.03	6.49E−04	0.07	−0.01	0.04	8.06E−01	0.07	9.16E−03	0.05	0.02	0.00	Skin tanning
rs2626547	*ZNF341*	20	32.40	A	G	0.91	−0.06	0.03	2.21E−02	0.92	−0.05	0.04	2.11E−01	−0.06	9.22E−03	0.91	0.50	0.36	Skin tanning
rs6060246	*TRPC4AP*	20	33.70	G	A	0.07	0.03	0.03	2.77E−01	0.09	0.13	0.04	3.37E−03	0.07	9.28E−03	0.09	0.09	0.17	Skin tanning
rs2747561	*PXMP4*	20	32.37	T	C	0.37	0.03	0.02	9.03E−02	0.35	0.05	0.02	3.30E−02	0.04	9.31E−03	0.31	0.34	0.83	Skin tanning
rs6060245	*TRPC4AP*	20	33.70	G	A	0.07	0.03	0.03	2.80E−01	0.09	0.13	0.04	3.37E−03	0.07	9.40E−03	0.09	0.09	0.17	Skin tanning
rs6058185	*TRPC4AP*	20	33.70	G	A	0.07	0.03	0.03	2.80E−01	0.09	0.13	0.04	3.37E−03	0.07	9.40E−03	0.09	0.09	0.60	Skin tanning
rs1890364	*EXOC2*	6	0.71	T	G	0.08	−0.07	0.03	3.02E−02	0.08	−0.06	0.04	1.52E−01	−0.06	9.40E−03	0.10	0.27	0.49	Skin tanning
rs117002968	*GRM5*	11	88.60	C	T	0.07	0.11	0.03	6.91E−04	0.07	−0.01	0.04	8.18E−01	0.07	9.48E−03	0.05	0.02	0.01	Skin tanning
rs10831539	*GRM5*	11	88.60	C	T	0.07	0.11	0.03	6.91E−04	0.07	−0.01	0.04	8.18E−01	0.07	9.48E−03	0.05	0.02	0.01	Skin tanning
rs317137	*NOX4*	11	89.16	C	T	0.55	0.04	0.02	2.21E−02	0.56	0.03	0.02	2.13E−01	0.03	9.51E−03	0.58	0.36	0.53	Skin tanning
rs2788223	*EXOC2*	6	0.72	G	A	0.07	−0.08	0.03	1.37E−02	0.08	−0.04	0.04	3.05E−01	−0.07	9.53E−03	0.10	0.20	0.55	Skin tanning
rs10738470	*BNC2*	9	16.94	T	C	0.09	0.05	0.03	9.57E−02	0.07	0.10	0.05	2.71E−02	0.06	9.61E−03	0.10	0.17	0.32	Skin tanning
rs4961508	*BNC2*	9	16.94	T	C	0.09	0.05	0.03	9.57E−02	0.07	0.10	0.05	2.71E−02	0.06	9.61E−03	0.10	0.17	0.32	Skin tanning
rs7861272	*BNC2*	9	16.94	G	C	0.09	0.05	0.03	9.57E−02	0.07	0.10	0.05	2.71E−02	0.06	9.61E−03	0.10	0.17	0.32	Skin tanning
rs55999610	*BNC2*	9	16.94	TA	T	0.09	0.05	0.03	9.57E−02	0.07	0.10	0.05	2.71E−02	0.06	9.61E−03	0.90	0.83	0.68	Skin tanning
rs1538587	*BNC2*	9	16.94	C	G	0.09	0.05	0.03	9.64E−02	0.07	0.10	0.05	2.71E−02	0.06	9.69E−03	0.10	0.17	0.32	Skin tanning
rs2626562	*ZNF341*	20	32.41	A	G	0.91	−0.06	0.03	2.40E−02	0.92	−0.06	0.04	2.05E−01	−0.06	9.69E−03	0.91	0.52	0.37	Skin tanning
rs17092297	*TRPC4AP*	20	33.70	A	G	0.07	0.03	0.03	2.80E−01	0.09	0.13	0.04	3.66E−03	0.07	9.74E−03	0.09	0.09	0.59	Skin tanning
rs11021471	*GRM5*	11	88.56	C	T	0.16	0.07	0.02	1.29E−03	0.15	0.00	0.03	9.14E−01	0.05	9.87E−03	0.13	0.03	0.06	Skin tanning
rs2207355	*PXMP4*	20	32.37	T	C	0.39	0.02	0.02	1.40E−01	0.37	0.06	0.02	1.56E−02	0.04	9.87E−03	0.33	0.34	0.81	Skin tanning
rs62068676	*SPG7*	16	89.65	T	C	0.11	0.04	0.03	1.43E−01	0.11	0.09	0.04	1.51E−02	0.06	9.87E−03	0.11	0.08	0.01	Skin tanning
rs7875833	*BNC2*	9	16.94	G	T	0.09	0.05	0.03	1.01E−01	0.07	0.10	0.05	2.59E−02	0.06	9.93E−03	0.10	0.17	0.32	Skin tanning
rs10810689	*BNC2*	9	16.94	T	A	0.09	0.05	0.03	1.01E−01	0.07	0.10	0.05	2.59E−02	0.06	9.93E−03	0.10	0.17	0.32	Skin tanning
rs10810691	*BNC2*	9	16.94	T	C	0.09	0.05	0.03	1.01E−01	0.07	0.10	0.05	2.59E−02	0.06	9.93E−03	0.10	0.17	0.31	Skin tanning
rs598952	*GRM5*	11	88.59	A	T	0.69	0.06	0.02	1.27E−03	0.70	0.00	0.03	8.93E−01	0.04	9.95E−03	0.25	0.70	0.31	Skin tanning

All SNPs with $P < 0.01$ are shown.

Abbreviations: AFR, African; CHR, chromosome; EA: effect allele; EAF: effect allele frequency; EAS, East Asian; EUR, European; JD, Jidong cohort; MB, megabase; META, meta analysis; NSPT, National Survey of Physical Traits cohort; OA: other allele.